The Plant Cell, Vol. 28: 1182–1199, May 2016, www.plantcell.org

A Nucleus-Encoded Chloroplast Phosphoprotein Governs Expression of the Photosystem I Subunit PsaC in *Chlamydomonas reinhardtii*

Damien Douchi,[a] Yujiao Qu,[b] Paolo Longoni,[a] Linnka Legendre-Lefebvre,[a] Xenie Johnson,[c,1] Christian Schmitz-Linneweber,[b] and Michel Goldschmidt-Clermont[a,2]

[a] Department of Botany and Plant Biology and Department of Molecular Biology, University of Geneva, 1211 Geneva 4, Switzerland
[b] Institute of Biology, Molecular Genetics, Humboldt University of Berlin, D-10115 Berlin, Germany
[c] Unité Mixte de Recherche 7141, CNRS/Université Pierre et Marie Curie, Institut de Biologie Physico-Chimique, 75005 Paris, France

ORCID IDs: 0000-0002-6155-9153 (D.D.); 0000-0002-9030-3528 (Y.Q.); 0000-0003-0587-7621 (P.L.); 0000-0003-1224-5868 (M.G.-C.)

The nucleo-cytoplasmic compartment exerts anterograde control on chloroplast gene expression through numerous proteins that intervene at posttranscriptional steps. Here, we show that the *maturation of psaC* mutant (*mac1*) of *Chlamydomonas reinhardtii* is defective in photosystem I and fails to accumulate *psaC* mRNA. The *MAC1* locus encodes a member of the Half-A-Tetratricopeptide (HAT) family of super-helical repeat proteins, some of which are involved in RNA transactions. The Mac1 protein localizes to the chloroplast in the soluble fraction. *MAC1* acts through the 5′ untranslated region of *psaC* transcripts and is required for their stability. Small RNAs that map to the 5′end of *psaC* RNA in the wild type but not in the *mac1* mutant are inferred to represent footprints of *MAC1*-dependent protein binding, and Mac1 expressed in bacteria binds RNA in vitro. A coordinate response to iron deficiency, which leads to dismantling of the photosynthetic electron transfer chain and in particular of photosystem I, also causes a decrease of Mac1. Overexpression of Mac1 leads to a parallel increase in *psaC* mRNA but not in PsaC protein, suggesting that Mac1 may be limiting for *psaC* mRNA accumulation but that other processes regulate protein accumulation. Furthermore, Mac 1 is differentially phosphorylated in response to iron availability and to conditions that alter the redox balance of the electron transfer chain.

INTRODUCTION

The photosynthetic electron transfer chain in the thylakoid membrane comprises several large pigment-protein complexes that function together with remarkable efficiency to convert light energy into chemical energy, which is in turn used to fuel metabolism. The assembly of the complexes of the photosynthetic electron transfer chain requires the concerted expression of genes in two separate compartments: the nucleus and the chloroplast. These genes encode not only the subunits of the photosynthetic complexes, but also a large cohort of proteins that are required for gene expression and complex assembly.

Photosystem I is composed of 12 to 19 polypeptide subunits, depending on the organism, that bind ~200 pigments and co-factors. In *Chlamydomonas reinhardtii*, four components of PSI are encoded in the chloroplast: the larger PsaA and PsaB subunits, as well as the smaller PsaC and PsaJ subunits (Redding, 2009). Ten other polypeptides are encoded in the nucleus and imported into the chloroplast where they assemble with the chloroplast-encoded subunits. Two other chloroplast-encoded proteins, Ycf3 and Ycf4, facilitate the assembly of the PSI complex (Boudreau et al., 1997; Naver et al., 2001; Ozawa et al., 2009). The expression of the chloroplast *psaA* and *psaB* genes is governed at the posttranscriptional level by a set of nucleus-encoded factors that are transcript specific. The *psaA* mRNA is assembled in two steps of *trans*-splicing from three separate precursors (Choquet et al., 1988; Kück et al., 1987). *Trans*-splicing of *psaA* depends on a chloroplast-encoded RNA, *tscA*, and at least 14 nucleus-encoded proteins (Goldschmidt-Clermont et al., 1990, 1991). The stability and translation of *psaA* mRNA further depends on Taa1, a nucleus-encoded member of the OPR family (octatrico peptide repeat) of RNA binding helical-repeat proteins (Lefebvre-Legendre et al., 2015). The stability and translation of *psaB* mRNA depend on Tab1, another OPR protein, and on Tab2, a protein that is widely conserved in oxygenic phototrophs but has no previously described RNA binding motifs (Dauvillee et al., 2003; Rahire et al., 2012; Stampacchia et al., 1997).

The expression of chloroplast genes encoding subunits of the other photosynthetic complexes similarly depends on numerous transcript-specific nucleus-encoded proteins. Likewise in flowering plants, a large group of nucleus-encoded proteins govern chloroplast gene expression at the levels of transcript processing, splicing and stability, C-to-U editing, and mRNA translation (Stern et al., 2010; Barkan, 2011). The somewhat surprising complexity of chloroplast gene expression and the large number of nuclear

[1] Current address: CEA, Direction des Sciences du Vivant, Institut de Biologie Environnementale et de Biotechnologie, Laboratoire de Bioénergétique et Biotechnologie des Bactéries et Microalgues, CEA Cadarache, Saint-Paul-lez-Durance, F-13108 France. CNRS, UMR Biologie Végétale et Microbiologie Environnementale, Saint-Paul-lez-Durance, F-13108 France. Aix Marseille Université, Laboratoire de Bioénergétique et Biotechnologie des Bactéries et Microalgues, Saint-Paul-lez-Durance, F-13108 France.
[2] Address correspondence to michel.goldschmidt-clermont@unige.ch.
The author responsible for distribution of materials integral to the findings presented in this article in accordance with the policy described in the Instructions for Authors (www.plantcell.org) is: Michel Goldschmidt-Clermont (michel.goldschmidt-clermont@unige.ch).
www.plantcell.org/cgi/doi/10.1105/tpc.15.00725

genes involved raises the question of whether this provides a route for regulation of the plastid by the nucleus. Alternatively it has been argued that part of the complexity may have arisen in a process of constructive neutral evolution, where preexisting nucleus-encoded proteins can suppress new mutations that appear in the chloroplast (Maier et al., 2008; Gray et al., 2010; Lukes et al., 2011; Barkan and Small, 2014). A typical example where this might be the case is provided by the nucleus-encoded editing factors that make specific C-to-U changes in the sequence of chloroplast mRNAs at a posttranscriptional step (Schmitz-Linneweber et al., 2005a). Another example may come from the numerous factors that are required for splicing in trans of the *psaA* mRNA in Chlamydomonas (Lefebvre-Legendre et al., 2014). In these cases, the nucleus-encoded proteins could be needed constitutively and would not be involved in chloroplast gene regulation in the strict sense.

This does not exclude the possibility that some of the nucleus-encoded proteins do participate in the regulation of chloroplast gene expression in response to environmental or developmental cues. For example, in Chlamydomonas, nitrogen deprivation leads to rapid decrease in the amount of cytochrome b_6f complexes. This coordinate response involves the proteolytic degradation of its subunits and also of Mca1 and Tca1, nucleus-encoded proteins that determine the stability and translation of *petA* mRNA, which encodes the Cyt*f* subunit (Raynaud et al., 2007; Boulouis et al., 2011; Wei et al., 2014). The concerted response to nitrogen deprivation also involves other nucleus-encoded proteins that take part in the assembly of the complex and its hemes (Wei et al., 2014). An early response of Chlamydomonas to iron deprivation is the downregulation of PSI and the remodeling of its light-harvesting antenna (Moseley et al., 2002; Naumann et al., 2005). There is a concomitant downregulation of Taa1, which is required for the stability and translation of *psaA* (Lefebvre-Legendre et al., 2015).

Here, we describe the identification of Mac1, a nucleus-encoded protein that localizes to the chloroplast where it is required for the expression of *psaC*. Mac1 belongs to the TPR/HAT (tetratrico peptide repeat/half a tetratrico peptide) family of helical repeat proteins, whose members are involved in RNA transactions (Hammani et al., 2014). Mac1 acts through the 5′UTR (untranslated region) on the stability of *psaC*, and Mac1 protein expressed in bacteria binds RNA in vitro. The amount of Mac1 is regulated in response to iron deprivation. We present evidence that Mac1 is phosphorylated and that this posttranslational modification is modulated by iron availability and other environmental conditions.

RESULTS

Identification of *MAC1*

A collection of random insertional mutants of Chlamydomonas was previously generated by transformation with an expression cassette containing the *aphVIII* gene, which confers paromomycin resistance (Johnson et al., 2010; Houille-Vernes et al., 2011). The mutants were screened for defects in photosynthesis based on chlorophyll fluorescence induction kinetics (Figure 1A). One of these mutants, which had an apparent defect in PSI and could not grow photoautotrophically, was chosen for further study. Immunoblotting with antibody against the PsaA subunit of PSI, which accumulated in the mutant to less than 30% of the wild-type level, confirmed that the mutant has a defect in PSI (Figure 1B). The loss of one subunit of a photosynthetic complex can lead to the degradation of the other subunits. This applies in particular to chloroplast mutants lacking PsaC (Takahashi et al., 1991). To investigate which subunit is primarily affected in the PSI-deficient mutant, wild-type and mutant RNA were analyzed by agarose gel electrophoresis and blot hybridization with probes for the chloroplast genes encoding three major subunits of PSI, *psaA*, *psaB*, and *psaC* (Figure 1C). This revealed a defect in the accumulation of *psaC* transcripts in the mutant. The *psaC* gene is upstream of *petL*, with which it is cotranscribed in the Chlamydomonas chloroplast genome. The slower migrating band is the dicistronic *psaC-petL* RNA (1.1 kb), while the faster migrating band is the monocistronic *psaC* RNA (0.45 kb) (Takahashi et al., 1991). Both of these transcripts were missing in the mutant, while the monocistronic *petL* RNA was present at elevated levels relative to the wild type (Figure 1C). By contrast, *psaA* was *trans*-spliced normally and *psaB* mRNA accumulated to wild-type levels. Because of its specific defect in the accumulation of *psaC* RNA, the mutant was called *mac1* (*mRNA of psaC*). For further analysis, the *mac1* mutant was backcrossed three times to the wild type. The wild-type and *mac1* progeny segregated 2:2, indicating a nuclear mutation, and paromomycin sensitivity or resistance segregated with the wild-type or PSI-deficient phenotype respectively in 92 progeny from 24 tetrads (some of them incomplete), suggesting that the *aphVIII* insertion was linked to the *mac1* mutation.

To identify the site of the *aphVIII* insertion in the *mac1* mutant, reverse PCR and sequencing were used to obtain a flanking sequence tag, which corresponded to gene Cre09.g389615 (g9646.t1) in Version 11 of the Phytozome database (https://phytozome.jgi.doe.gov/pz/portal.html). The insertion mapped to exon 2 of the predicted gene (Supplemental Figure 1), and *mac1* is thus most likely a null mutant. Genomic transformation with both BAC clone 23A16 and a 5.6-kb subclone (*pMAC1_gen3*) containing the Cre09.g389615 gene efficiently rescued the photosynthetic deficiency of *mac1* (Supplemental Figure 2). In representative complemented transformants, the accumulation of the PsaC protein and the *psaC* transcripts were restored (Figures 2A and 2B). Thus, mapping of the insertion site and complementation with the wild-type gene identified Cre09.g389615 as the *MAC1* gene. To raise a rabbit antiserum against Mac1, a C-terminal domain of the protein was expressed in *Escherichia coli*. Although the serum recognized Mac1, it was not monospecific and also recognized several nonspecific bands including one that nearly comigrated with Mac1 (Figure 2B) or could sometimes barely be resolved (Figure 2C, marked with an asterisk). Therefore, to facilitate the detection of Mac1, the *MAC1* gene was tagged with a triple hemagglutinin (HA) epitope (*MAC1-HA*). This construct rescued the *mac1* mutant with high efficiency (Figures 2A and 2B; Supplemental Figure 2), showing that Mac1-HA is functional. As expected, the HA-tagged protein was also detected by the Mac1 antiserum and migrated more slowly than the untagged form (Figure 2B, *mac1;MAC1-HA*).

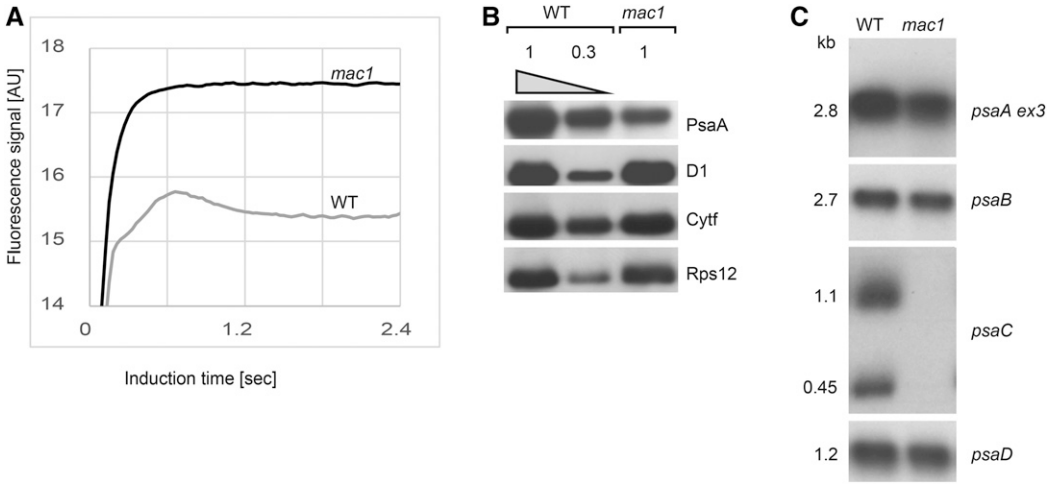

Figure 1. Characterization of the *mac1* Mutant.

(A) The induction of chlorophyll fluorescence in the wild type and the *mac1* mutant was monitored upon a transition from dark to light using a video imaging system. The cells were grown in the dark on a plate containing acetate medium.

(B) Total protein extracts of the wild type (25 μg [1] and 8 μg [0.3]) and of the *mac1* mutant (25 μg) were analyzed by SDS-PAGE and immunoblotting with antisera against the proteins indicated on the right (PsaA subunit of PSI, D1 [PsbA] subunit of PSII, CytF [PetA] subunit of the cytochrome b_6f complex, and Rps12 subunit of the chloroplast ribosome as a loading control).

(C) RNA extracts of the wild type and of the *mac1* mutant were analyzed by denaturing gel electrophoresis, blotting to nylon membranes, and hybridization with the radiolabeled probes indicated on the right. The sizes of the transcripts are shown on the left.

MAC1 encodes a predicted polypeptide of 982 amino acids. A striking feature of the predicted Mac1 polypeptide is the presence of two adjacent domains each with six or seven tetratricopeptide (TPR) repeats, most of which have features of the HAT subfamily (Half-A-TPR) (Supplemental Figure 1C). Members of this subfamily are implicated in RNA metabolism and some have been shown to associate with RNA in vivo or to bind RNA in vitro (Hammani et al., 2012, 2014; Loizeau et al., 2014). Indeed, we found the closest paralog of Mac1 in Chlamydomonas to be Mbb1, a TPR/HAT repeat protein involved in the stabilization or maturation of the *psbB/T* and *psbH* mRNAs (Vaistij et al., 2000a; Loizeau et al., 2014) (Supplemental Figure 3 and Supplemental Data Set 1). The ortholog of Mbb1 in vascular plants, HCF107, is required for the stability of *psbH* transcripts (Felder et al., 2001; Sane et al., 2005; Hammani et al., 2012).

Mac1 Is a Chloroplast Protein

Immunofluorescence and confocal microscopy were used to determine the subcellular localization of Mac1. In the *mac1*; *MAC1-HA* strain, immunolabeling with a monoclonal anti-HA antibody gave a signal in the chloroplast, which was absent in the wild-type control (Figure 3; Supplemental Figure 4). The chloroplast localization of Mac1-HA was confirmed by colabeling with a polyclonal antibody against the chloroplast stromal protein DnaK. Furthermore, the localization of Mac1-HA was distinct from that of Rpl37 (Figure 3A) and Rpl4 (Supplemental Figure 4), subunits of cytoplasmic ribosomes.

Cell fractionation experiments were used to confirm the localization of Mac1. The rabbit polyclonal antibody against the Mac1 protein was used to probe immunoblots of Chlamydomonas subcellular fractions (Figure 3B). Mac1 was found in the chloroplast fraction, together with the chloroplast markers PsaC and DnaK, but not in the supernatant of the lysate which contained the Rpl37 subunit of the cytosolic ribosomes. Further fractionation of the chloroplasts yielded a stromal fraction with soluble proteins such as DnaK and a membrane pellet, which contained the PsaC subunit of PSI, an integral protein of the thylakoid membrane. The Mac1 protein cofractionated with DnaK in the soluble fraction and showed no indication of membrane association.

To investigate whether Mac1 is part of a ribonucleoprotein complex, an extract of total soluble proteins was prepared from a strain expressing HA-tagged Mac1 (*mac1*;*MAC1-HA*). Half of the extract was treated with RNase, while the rest was mock-treated, and then the two samples were fractionated by sucrose gradient sedimentation (Figure 3C). Most of Mac1 remained close to the top of the gradient, in a position consistent with the expected sedimentation of the monomer. A minor fraction of Mac1 was distributed in larger complexes. Their sedimentation was not significantly affected by the RNase treatment.

Mac1 Is Required for *psaC* RNA Stability

The absence of detectable *psaC* transcripts in *mac1* could be due to a defect either in transcription or in RNA stability. To distinguish between these two possibilities, transcription of *psaC* was evaluated in run-on transcription assays. Wild-type and *mac1* cells were permeabilized and incubated with radiolabeled [α-^{32}P]UTP for 5 or 15 min to allow extension of nascent transcripts (Klinkert et al., 2005). Under such conditions, there is no transcription reinitiation and the amount of radiolabel incorporated in nascent transcripts reflects the density of transcribing polymerases on the

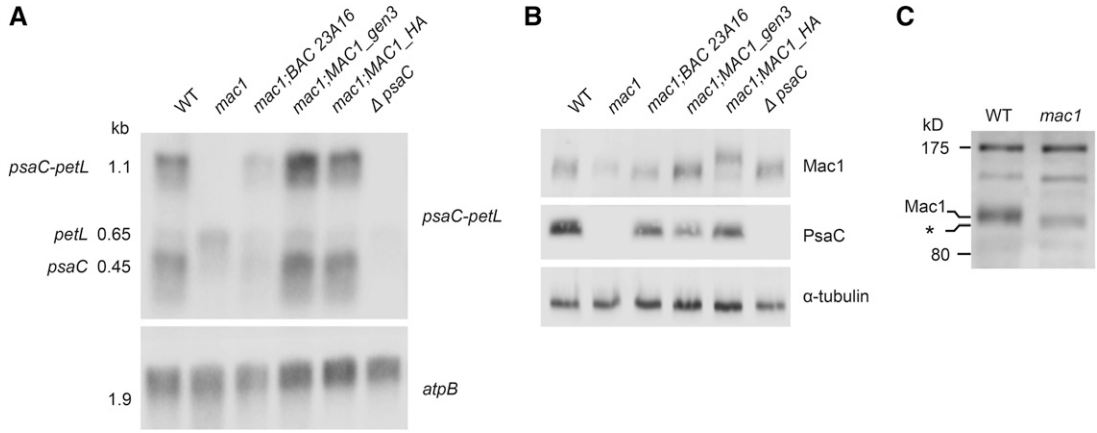

Figure 2. Complementation of the *mac1* Mutant.

(A) RNA gel blot hybridization analysis of the *mac1* mutant and complemented strains. RNA was extracted from the wild type, the *mac1* mutant, the *mac1* mutant rescued by transformation with the genomic BAC clone (*BAC23A16*), with the genomic subfragment containing *MAC1* (p*MAC1_gen3*), or with a derivative of the latter carrying a triple HA epitope (*MAC1-HA*), and a chloroplast mutant with an insertion in the *psaC* gene (*ΔpsaC*). The samples were analyzed by denaturing gel electrophoresis and RNA gel blot hybridization with radiolabeled fragments containing *psaC* and *petL* (upper panel) or *atpB* as a control (lower panel). The sizes of the transcripts are shown on the left (1.1 kb, *psaC-petL*; 0.65 kb, *petL*; 0.45 kb, *psaC*).
(B) Immunoblot analysis of total proteins extracts from the same strains as in **(A)**. The antisera used for immunoblotting are shown on the right.
(C) Specificity of the antiserum against Mac1. Total protein extracts of the wild type and of the *mac1* mutant were analyzed by SDS-PAGE and immunoblotting with a rabbit polyclonal antiserum raised against recombinant Mac1. A minor nonspecific band that is present in the mutant (marked with an asterisk) runs just below Mac1.

respective gene (Guertin and Bellemare, 1979; Monod et al., 1992). The radiolabeled RNA was extracted and hybridized to DNA probes spotted on a nylon membrane (Figure 4). There was no significant difference in the radioactive signal for *psaC* between the *mac1* mutant and the wild type. These results indicate that transcription of *psaC* proceeds at normal rates in *mac1* and, hence, that it is the stability of *psaC* RNA that is compromised in the mutant.

Some helical-repeat proteins are known to stabilize specific chloroplast mRNAs by tightly binding to defined sequences in the 5′UTR or the 3′UTR and protecting the target transcript against exonucleases (Pfalz et al., 2009; Prikryl et al., 2011). This mechanism can lead to the accumulation of RNA footprints, small RNA fragments that are protected by the respective RNA binding proteins (Pfalz et al., 2009; Ruwe and Schmitz-Linneweber, 2012; Zhelyazkova et al., 2012; Loizeau et al., 2014). Footprints that map to the 5′end of the *psaC* transcripts could be identified in Chlamydomonas small RNA databases (Figure 5; Supplemental Figure 5). This was confirmed by RNA blot hybridization, which detected a small RNA of ~50 nucleotides that was present in the wild type, but absent in the *mac1* mutant (Figure 5B, marked with an arrow). This suggests that Mac1 may bind the 5′end of the *psaC* transcripts or may indirectly promote the binding of a protein to this transcript, two alternatives that are not mutually exclusive.

Mac1 Acts through the 5′UTR of *psaC* RNAs

Mbb1, the closest paralog of Mac1 in Chlamydomonas, protects the *psbB* transcript by associating with its 5′UTR (Vaistij et al., 2000b; Loizeau et al., 2014). This precedent and the presence of Mac1-dependent footprints matching the 5′ end of *psaC* transcripts suggest that the target of Mac1 may be the 5′UTR of *psaC*. To test this hypothesis, a chimeric reporter gene was constructed (*psaC:lucCP*) with the promoter and 5′UTR of *psaC* fused to the coding sequence of firefly luciferase (Matsuo et al., 2006) followed by the 3′UTR of *rbcL*. For biolistic chloroplast transformation, the chimeric luciferase reporter was introduced in the atpB-INT vector (Michelet et al., 2011), which carries a modified *atpB* gene as selectable marker, allowing selection of photoautotrophic transformants in a *ΔatpB* mutant host (Figure 6). The strain with the *psaC:lucCP* reporter was then crossed to the *mac1* mutant, so that sibling progeny with either the wild-type or the *mac1* nuclear genome were recovered for analysis. Luciferase activity in the *mac1* mutant (*mac1/psaC:lucCP*) was at background level and, thus, at least 30-fold lower than in the wild type (Figure 6B). Luciferase activity was restored to wild-type levels by transforming the *mac1/psaC:lucCP* progeny with the wild-type *MAC1* gene (*mac1;MAC1/psaC:lucCP*). The *mac1* mutation did not significantly affect the expression of a control reporter with the *psaB* promoter and 5′UTR (*mac1/psaB:lucCP*). Luciferase expression with the *psaB* construct was much stronger than with the *psaC* construct, but such differences between chimeric genes expressed in the chloroplast are commonly observed in Chlamydomonas (Michelet et al., 2011). The results indicate that a genetic target of Mac1 is found in the promoter or 5′UTR of *psaC*. Since the *mac1* mutation affects *psaC* transcript stability, it is most likely that the target of Mac1 is in fact in the 5′UTR rather than the promoter.

Mac1 Binds RNA in Vitro

To investigate the RNA binding properties of Mac1, a recombinant protein corresponding to the full sequence (except for the

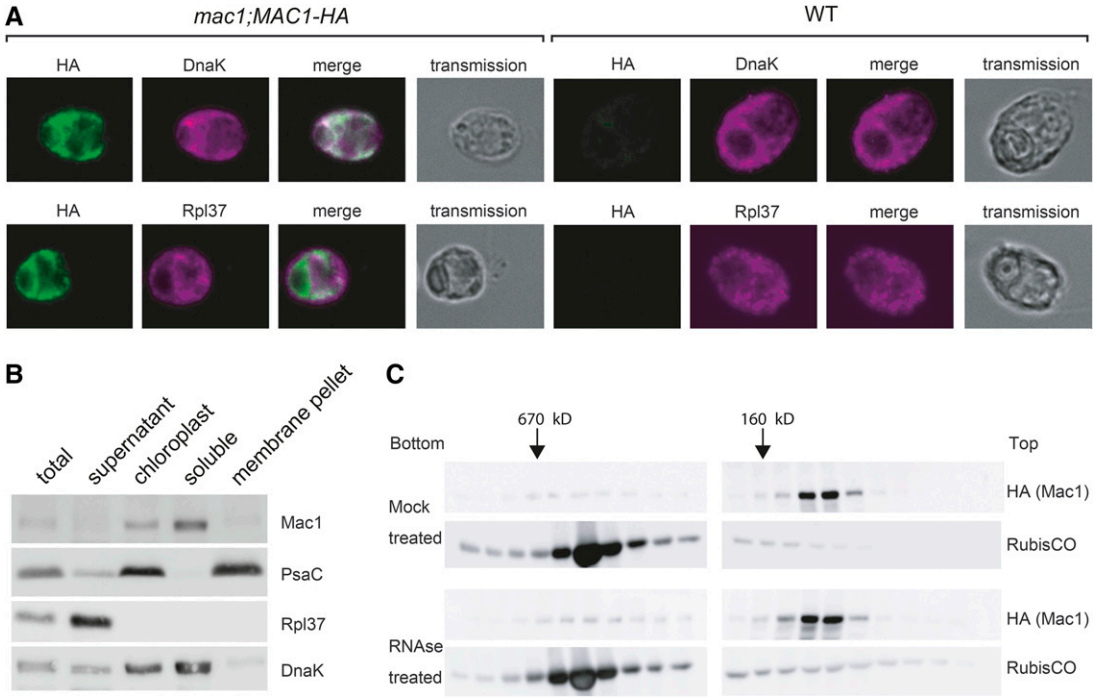

Figure 3. Mac1 Localizes to the Chloroplast.

(A) Immunofluorescence of Chlamydomonas *mac1* mutant cells complemented with an HA-epitope-tagged *MAC1* gene (*mac1;MAC1-HA*) or wild-type cells as a control, fixed in methanol to remove chlorophyll. The samples were decorated with both a monoclonal mouse antibody against the HA epitope and a rabbit polyclonal antibody against either the chloroplast protein DnaK or the cytosolic subunit of the ribosome Rpl37. The anti-mouse and anti-rabbit secondary antibodies were labeled with Alexafluor 647 or Alexafluor 546, respectively. Immunofluorescence was observed by confocal microscopy and is shown separately (green and magenta respectively) or as a merged image (green + magenta in white; third panels). An image of the same cells observed by transmission microscopy is also presented (fourth panels).

(B) Cells from the cell wall-deficient mutant *cw15* were lysed by nebulization. The lysate (total) was subjected to low-speed centrifugation and the supernatant was collected (supernatant) while the chloroplasts in the pellet were further purified by Percoll gradient centrifugation (chloroplast). The chloroplasts were further lysed by sonication and fractionated by high-speed centrifugation into a supernatant fraction (soluble) and a pellet (membrane pellet). Equal amounts of protein from each fraction were subjected to SDS-PAGE and immunoblotting with the polyclonal antisera indicated on the right.

(C) Sucrose gradient sedimentation analysis of Mac1. An extract of total soluble protein from the *mac1;MAC1-HA* strain was split in two aliquots, one was mock-treated and the other was treated with RNaseA. The protein complexes were then separated by sedimentation in sucrose density gradients. Twenty fractions were collected from the bottom and analyzed by SDS-PAGE and immunoblotting with either anti-HA monoclonal antibody or anti-Rubisco antiserum as indicated. The sedimentation of markers used for calibration in a parallel gradient is indicated at the top (thyroglobulin, 670 kD; aldolase, 160 kD). Rubisco holoenzyme has a molecular mass of ~550 kD.

predicted transit peptide) was expressed in *E. coli*, with a tag of six histidines at the C terminus. After nickel-affinity chromatography, the preparation still contained contaminants, some of which were found to also bind RNA in preliminary experiments. Therefore, the proteins were further separated by gel filtration chromatography (Figure 7). In the eluted fractions, recombinant Mac1 protein was identified by SDS-PAGE by its expected size (96 kD; Figure 7A) and its recognition by Mac1 antiserum in immunoblots (Figure 7B). Mac1 peaked in the fraction expected for a monomer of its size (lane 8). To assay RNA binding, a radiolabeled probe was prepared corresponding to 51 nucleotides at the 5′end of *psaC* mRNA, matching the footprint observed in vivo. For the electrophoretic mobility shift assay, aliquots of each protein fraction eluted from the gel filtration column were mixed with the radiolabeled probe, and the RNA-protein complexes that formed were separated from the unbound probe by nondenaturing gel electrophoresis. The major RNA-protein complex that formed matched exactly the elution profile of Mac1 protein, peaking in lane 8 (B_2, Figure 7C). Minor complexes (B_1 and B_3, Figure 7C) with other proteins were clearly separated from Mac1, peaking in fractions 5 and 12, respectively. Mac1 bound the RNA probe with high affinity. The estimated K_d was 40 to 60 nM for two independent preparations, comparable to the K_d observed in vitro for HCF107 (70 nM) (Hammani et al., 2012)

Regulation of Mac1 in Response to Iron Limitation

In Chlamydomonas, early responses to iron limitation under mixotrophic conditions involve the dismantling of the photosynthetic electron transfer chain, and in particular of PSI and the

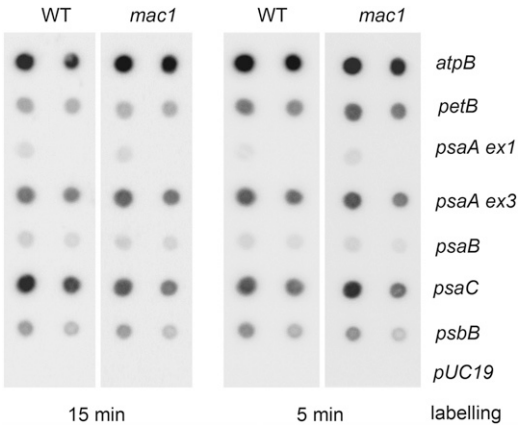

Figure 4. Analysis of *psaC* Transcription in the *mac1* Mutant.

For the run-on transcription assay, duplicate nylon membranes were decorated with spots of PCR fragments derived from the chloroplast genes indicated on the right (0.6 and 0.3 μg DNA of each probe, except a single spot of 0.25 μg for *psaA ex1*) or the bacterial plasmid vector *pUC19* as a negative control. Wild-type or mutant *mac1* cells were permeabilized by freezing and thawing and then radiolabeled with ^{32}P-UTP for 15 min (left panel) or 5 min (right panel). The labeled RNAs were extracted and hybridized to the membranes (the same pair of membranes was used first with the 5 min samples, and after stripping used again with the 15 min samples). In the run-on transcription assay elongating RNA polymerases insert radiolabel in the nascent transcript, but transcription initiation does not occur. The hybridization signal is thus a measure of the density of transcribing polymerases on the respective gene.

cytochrome b_6f complex (Moseley et al., 2002; Hohner et al., 2013). PsaC is the subunit of PSI that directly binds two of its three 4Fe4S iron-sulfur centers, F_A and F_B. To investigate whether the response to iron limitation also involves the regulation of Mac1 protein accumulation, *mac1/Mac1-HA* cultures were grown through 10 division cycles in acetate-containing medium at three different iron concentrations: 20 μM Fe (iron replete), 1 μM Fe (limited), and 0.2 μM Fe (deficient) (Glaesener et al., 2013). As expected, in the iron-deficient culture (0.2 μM Fe) PSI decreased approximately 4-fold as estimated from the reduced accumulation of PsaA and PsaC compared with a dilution series of proteins from the iron-replete culture (Figure 8A; Supplemental Figure 6). There was a concomitant ~50% decrease in the abundance of Mac1-HA (Supplemental Figure 6D). Similar results were obtained with a wild-type strain using the Mac1 antibody (Figure 8B). However the accumulation of ATP synthase was not reduced under iron limitation (Figure 8A, CF1 antiserum), confirming previous observations that the response to iron starvation is not a general dismantling of the thylakoid membrane (Moseley et al., 2002; Hohner et al., 2013). Under the same conditions, the abundance of the *psaC* transcripts decreased ~30% as estimated from a comparison to a dilution series of RNA from iron-replete conditions (Figure 8C; Supplemental Figure 6B). The amounts of *atpB* mRNA remained unchanged, indicating that the response is not a general degradation of chloroplast mRNA. The lack of PsaC protein in the *ΔpsaC* mutant (Takahashi et al., 1991) did not affect the accumulation of Mac1 (Figure 2B), suggesting that the decrease of Mac1 in iron-deficient conditions is not a consequence of the reduced levels of PsaC.

Under iron deficiency, we observed a concomitant decrease in Mac1-HA and *psaC* mRNA accumulation, with the former more pronounced than the latter (Supplemental Figures 6D and 6F). The question thus arises whether the amount of Mac1 could be limiting for *psaC* expression. To investigate this point, different transformants of *mac1* with the *MAC1:HA* construct, expressing different levels of Mac1-HA, were compared under iron-replete conditions (Figure 9). In strains that expressed different levels of Mac1-HA, the accumulation of the *psaC* transcripts paralleled the amounts of Mac1-HA (Figure 9A). However the amount of PsaC protein in the different transformants remained constant and similar to the wild type (Figure 9B). These observations suggested that Mac1-HA may be limiting for *psaC* mRNA accumulation, but that increased levels of *psaC* mRNA do not lead to increased accumulation of PsaC. This could be due to translational or posttranslational regulation of PsaC amounts.

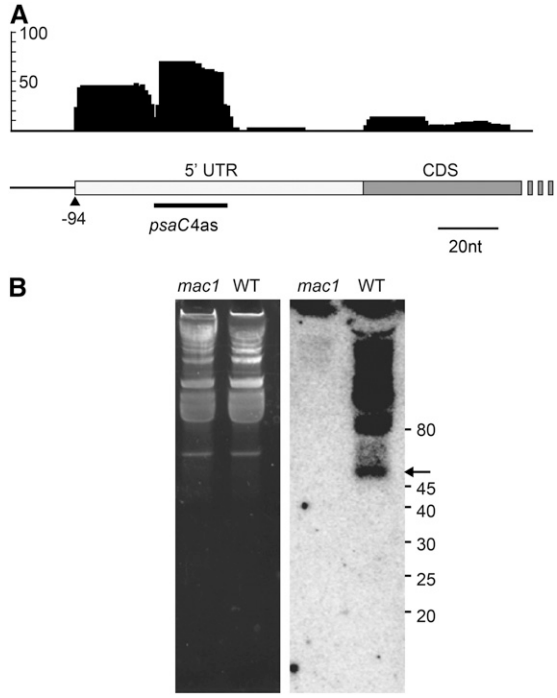

Figure 5. Small RNA Footprints in the 5′UTR of *psaC.*

(A) sRNA sequence coverage graph of the *psaC* 5′-region. Per-base read coverage within this region was extracted from sRNA sequencing databases (Ibrahim et al., 2010; Loizeau et al., 2014). Bars represent the *psaC* 5′UTR and the coding sequence (the actual sequence is provided in Supplemental Figure 5). The arrowhead marks the 5′-end of the *psaC* 5′UTR. A line labeled *psaC*4as denotes the antisense probe used in **(B)**.
(B) Low molecular weight enriched RNA extracted from the *mac1* mutant and the wild type was subjected to gel electrophoresis (left panel, ethidium bromide fluorescence image), transferred to nylon membranes, and hybridized with the radiolabeled antisense probe. The arrow marks a small RNA of ~50 bases that is present in the wild type but not in the *mac1* mutant.

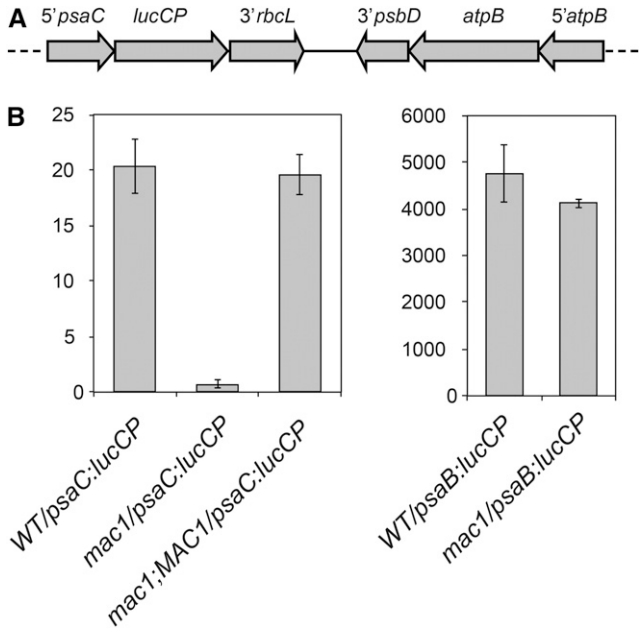

Figure 6. The 5′UTR of *psaC* Contains a Target of *MAC1*.

(A) Schematic map of the chimeric *psaC:lucCP:rbcL* reporter inserted in the chloroplast genome next to the *atpB* gene, which served as a selection marker for transformation of a *ΔatpB* host strain. In this construct, the *psaC* promoter and 5′UTR are fused to a codon-optimized coding sequence of the firefly luciferase, followed by the 3′UTR of *rbcL*. A similar construct where the *psaB* promoter and 5′UTR replace those of *psaC* was used as a control. In the atpB-INT transformation vector that was used, the 3′UTR of *atpB* has been replaced with the 3′UTR of *psbD* (Michelet et al., 2011).
(B) Luciferase assays of the Chlamydomonas strains indicated at the bottom. The nuclear genotype is indicated first, followed by a slash (/) and the chloroplast genotype. Nuclear genotypes: WT, wild type; *mac1*, *mac1* mutant line; *mac1;MAC1*, *mac1* mutant line complemented with the *MAC1* gene. Chloroplast genotypes: *psaC:lucCP*, chimeric *psaC:lucCP:rbcL* reporter; *psaB:lucCP*, chimeric *psaB:lucCP:rbcL* reporter. Three independent lines of each genotype were assayed in three technical replicates (luminescence is indicated with arbitrary units, error bars represent the SE of the three lines).

Phosphorylation of Mac1

Phosphorylation is a posttranslational modification that is involved in the regulation of numerous proteins. To analyze whether Mac1 could be subject to protein phosphorylation, protein extracts of *mac1*;*MAC1-HA* were analyzed using electrophoresis in polyacrylamide gels containing a Phos-tag gradient (Phos-tag PAGE; Supplemental Figure 7). When chelated with a divalent cation such as Zn^{2+}, Phos-tag binds phosphate groups and retards the migration of phosphorylated polypeptides (Kinoshita et al., 2006; Kinoshita and Kinoshita-Kikuta, 2011; Longoni et al., 2015). Immunoblotting with monoclonal anti-HA antibody revealed two bands for Mac1, suggesting that the upper one (P_1) could represent phosphorylated Mac1 (Figure 10). Treatment of the sample with λ protein-phosphatase led to the disappearance of the slowly migrating band, confirming that it corresponds to a phosphorylated form of Mac1. As a control, a strain expressing HA-tagged Sedoheptulose Bis Phosphatase (Sbp-HA) (Loizeau et al., 2014) was analyzed in parallel and there was no evidence that this protein was phosphorylated.

The availability of iron had a strong effect on the phosphorylation of Mac1 (Figure 10B). In cells grown under iron-replete mixotrophic conditions, Mac1 was strongly phosphorylated. After growth under conditions of iron limitation, the ratio of phosphorylated (P_1) to nonphosphorylated Mac1 (U) decreased and was even lower under iron depletion. As already observed in the previous section (Figure 8), the total amount of Mac1-HA concomitantly decreased under iron depletion compared with iron sufficiency. To control for the possibility that the lower apparent ratio of phosphorylation, which paralleled the reduction in the total amount of Mac1, could be due to an artifact of Phos-tag PAGE and immunoblotting, a dilution series of the sample from iron-replete condition was similarly analyzed (Figure 10C). The ratio of the phosphorylated band to the unphosphorylated form did not change significantly at lower total protein concentrations, thus corroborating the validity of the observation that phosphorylation of Mac1-HA is lower under iron limitation.

Phosphorylation of light-harvesting complex II (LHCII) subunits in the thylakoid membrane by the kinase Stt7 is regulated by the redox state of the electron transfer chain (Lemeille and Rochaix, 2010). Under anaerobic conditions in the dark, which lead to a reduction of the plastoquinone pool (state 2), Mac1-HA was largely phosphorylated (Figure 10D, lane 2). The two slowly migrating bands (labeled P_1 and P_2) could represent different degrees of phosphorylation of Mac1. Conversely under aerobic conditions in low light, which favor plastoquinone oxidation (state 1), Mac1 was partly unphosphorylated (Figure 10D, lane 1, band labeled U). To determine whether this phosphorylation depends on the Stt7 kinase, the *MAC1:HA* construct was transformed into the *stt7-7* mutant. In this strain, the phosphorylation patterns of Mac1-HA in state 1 and state 2 conditions were the same as in the wild-type *MAC1:HA* strain, indicating that Stt7 is not involved in the phosphorylation of Mac1 (Figure 10D, lanes 3 and 4).

Proteomic surveys of Chlamydomonas protein phosphorylation have indicated that Mac1 can be phosphorylated at serines 137 and 139 (Wang et al., 2014). To determine whether these are the residues that account for the phosphorylation of Mac1 detected by Phos-tag electrophoresis, a mutant version of *MAC1-HA* in which both serines 137 and 139 were replaced by alanines was constructed, *MAC1-AA-HA*. The *mac1* mutant strain transformed with *MAC1-AA-HA* grew normally on minimal medium, indicating that the modified protein is functional. The migration of phosphorylated Mac1-AA-HA in Phos-tag gels was unaffected compared with wild-type Mac1-HA in state 1 or state 2 conditions (Figure 10D, lanes 5 and 6), indicating that the major sites of phosphorylation that can be detected in this way are not serines 137 or 139.

DISCUSSION

Mac1 Controls the Stability of *psaC* mRNA

Mac1 was identified through the analysis of a nonphotosynthetic mutant deficient for PSI. The primary defect in *mac1* is its failure to accumulate *psaC* mRNA (Figures 1C and 2A) and the PsaC

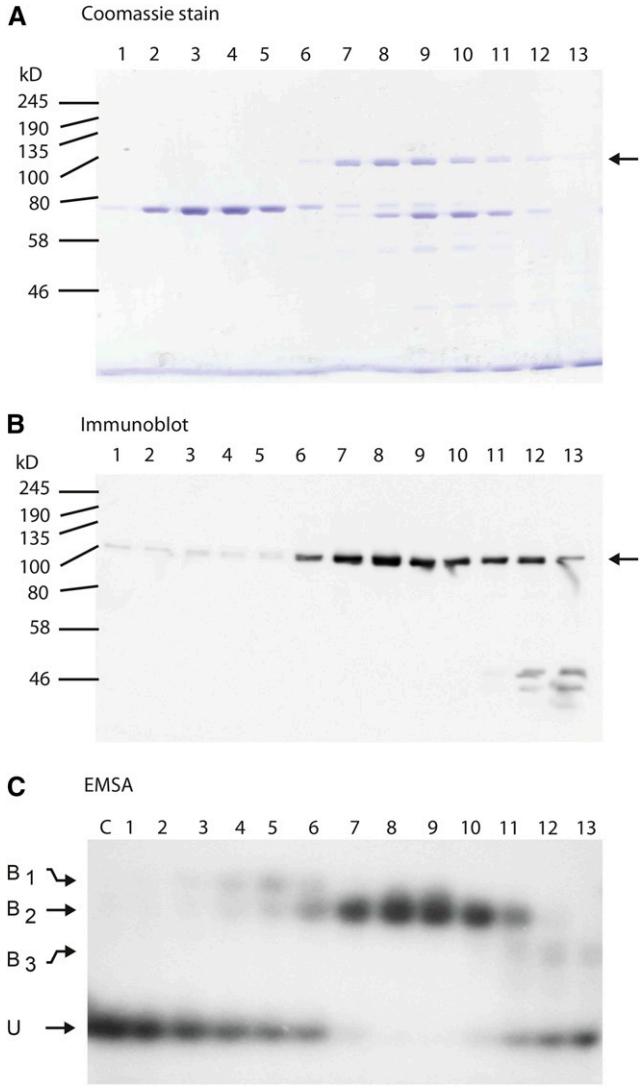

Figure 7. Mac1 Binds RNA in Vitro.

(A) Following Ni-NTA affinity chromatography, Mac1 was further purified by gel filtration chromatography. Selected fractions were analyzed by SDS-PAGE and staining with Coomassie Brilliant Blue R 250. The band corresponding to Mac1 is indicated with an arrow.

(B) The same fractions as in **(A)** were analyzed by SDS-PAGE and immunoblotting with Mac1 antibody.

(C) The same fractions as in **(A)** and **(B)** were used for electrophoretic mobility shift assays with a radiolabeled RNA probe corresponding to the first 51 nucleotides from the 5′UTR of *psaC* mRNA. The positions of three RNA-protein complexes (B_1, B_2, and B_3) and the unbound RNA (U) are indicated on the left. The peak fractions that form the major complex (B_2) coincide with the peak of elution of Mac1 centered on lane 8. The free probe was run alongside in lane C.

subunit (Figure 2B). This has ensuing consequences on the accumulation of PsaA (Figure 1B) and presumably other PSI subunits, which are known to be destabilized in the absence of PsaC (Takahashi et al., 1991). Mac1 localizes to the chloroplast, where it is found in the soluble, stromal fraction (Figure 3).

In the chloroplast genome of Chlamydomonas, *psaC* is transcribed in a polycistronic unit that also contains the downstream *petL* gene (Takahashi et al., 1994). In the *mac1* mutant, the accumulation of the monocistronic *psaC* mRNA and the dicistronic *psaC-petL* transcript are specifically affected, while the amount of monocistronic *petL* mRNA is slightly elevated. This suggests that the *mac1* mutation affects the stability rather than the transcription of *psaC*. Indeed, in a run-on transcription assay the activity of *psaC* appeared comparable in the mutant and in the wild type (Figure 4). Furthermore, a fragment containing the promoter and 5′UTR of *psaC* was sufficient to confer dependence on *MAC1* to a chimeric *psaC-lucCP* luciferase reporter (Figure 6). Although an accessory effect on transcription cannot be ruled out, taken together these results indicate that Mac1 is involved, directly or indirectly, in stabilizing transcripts containing *psaC* through its 5′UTR. This interpretation is supported by the identification in existing databases of small RNAs (sRNA) corresponding to the 5′ end of the *psaC* transcripts. Using RNA gel blot hybridization, the existence of a sRNA from *psaC* (approximately 50 nucleotides) could be confirmed in vivo and was shown to depend on the presence of Mac1 (Figure 5). Such sRNA footprints were first identified in plant chloroplasts at the position of RNA binding proteins such as PPR10, which protect the bound RNA against exonucleolytic degradation from both sides (Pfalz et al., 2009; Prikryl et al., 2011). Likewise in Chlamydomonas, small RNAs at the 5′end of *psbB* and *psbH* are formed in the presence of Mbb1, a nucleus-encoded protein that is required for the stable accumulation of the two mRNAs (Loizeau et al., 2014) and is the closest paralog of Mac1 (Supplemental Figure 3). Interestingly, HCF107, the ortholog of Mbb1 in *Arabidopsis thaliana* and maize (*Zea mays*), can bind *psbH* RNA in vitro and forms a sRNA footprint in vivo (Hammani et al., 2012). Mac1 is only found in Chlorophyta, whereas in maize, the pentatricopeptide repeat (PPR) protein CRP1 binds the 5′UTR of *psaC*, where it generates a sRNA footprint and is required for its efficient translation (Fisk et al., 1999; Schmitz-Linneweber et al., 2005b; Ruwe and Schmitz-Linneweber, 2012).

Mac1 contains two domains with tandem repeats of 34-amino acid residues that belong to the HAT/TPR family. Members of the HAT repeat proteins, which in turn belong to the helical-repeat superfamily, are involved in RNA interactions (Preker and Keller, 1998). Indeed, Mac1 protein expressed in bacteria binds RNA with high affinity in vitro (Figure 7). As mentioned above, HCF107 also belongs to this family and binds RNA in vitro with similar affinity (Hammani et al., 2012). In the PPR proteins, which form the most prevalent helical-repeat protein family in plant organelles (Barkan and Small, 2014), the 35-amino acid repeats are composed of two antiparallel α-helices that stack onto one another to form a superhelical backbone (Ke et al., 2013; Yin et al., 2013). Each modular repeat of a PPR protein interacts with one nucleotide of the bound RNA through specific residues that determine the recognition of the target base, allowing the definition of a "PPR code." The HAT repeats also form a superhelical scaffold, and it can be predicted that TPR/HAT domains of Mac1 will bind RNA in a similar way (Bai et al., 2007; Hammani et al., 2014). In the Chlamydomonas sRNA databases that we queried (Figure 5), a series of sRNAs corresponding to the 5′end of *psaC* delineate a relatively long footprint (approximately 50 nucleotides), which is roughly the size of the sRNA detected in vivo, and two

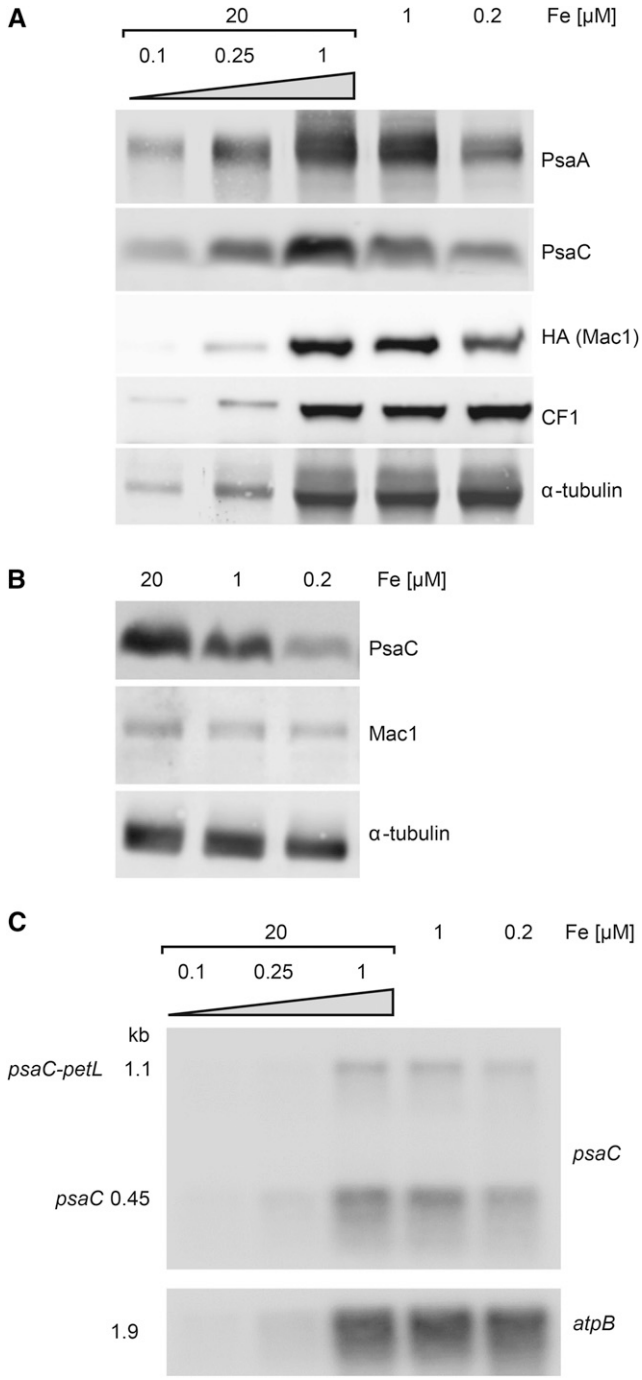

Figure 8. Mac1 and PsaC Levels Coordinately Respond to Iron Availability.

(A) Cultures of the *mac1* mutant complemented with an HA-epitope tagged *MAC1* gene (*mac1;MAC1-HA*) were grown mixotrophically (acetate-containing medium in the light) for 10 doublings in the presence of different concentrations of Fe: 20, 1, or 0.2 μM. Total cell extracts were analyzed by SDS-PAGE and immunoblotting with the antisera indicated on the right. A dilution series of the iron-replete sample (20 μM) is presented in the first three lanes.

(B) Wild-type cells were grown and analyzed as in **(A)**, and Mac1 was detected with the polyclonal antiserum (see Figure 2C).

(C) RNA was extracted from the same wild-type cultures as in **(B)** and subjected to denaturing gel electrophoresis and blot hybridization with radiolabeled probes for *psaC* (upper panel) or *atpB* as a control (lower panel).

subpopulations of shorter small RNAs map to the same region. There are two TRP/HAT domains in Mac1 (Supplemental Figure 1C), each of which consists of six or seven TRP repeats and is thus expected by analogy with PPR proteins to bind six to seven bases in the RNA (Barkan and Small, 2014). The relatively large size of the protected RNA fragment could be due to binding of two adjacent sites by the two TPR/HAT domains of Mac1 with a possible intervening RNA loop, such as was proposed for the binding of CRP1 to the *petB-petD* site in maize (Barkan et al., 2012). Alternatively, it is also possible that the large footprint is generated by one or more other partner proteins in a Mac1-dependent manner. It is conceivable that the minor fraction of Mac1 that sediments with large complexes in sucrose gradients could reflect its transient or labile association with other partners.

In Chlamydomonas, there are several examples of nucleus-encoded proteins that bind the 5′end of their respective target transcripts and offer protection against 5′ to 3′ exonucleolytic degradation. Apart from Mbb1, the closest paralog of Mac1 mentioned above, these also include the TPR/HAT protein Nac2, which is required to stabilize *psbD* RNA (Kuchka et al., 1989; Nickelsen et al., 1999). Other examples are provided by members of the OPR family of helical-repeat proteins, such as Taa1 and Tab1, which are required for the stability and translation of *psaA* and *psaB*, respectively, and Mbi1, which is necessary for the stable accumulation of *psbI* mRNA (Lefebvre-Legendre et al., 2015; Wang et al., 2015). Also of interest is another OPR protein, Mcg1, which is required for stabilization of *petG* mRNA and generates a corresponding sRNA footprint at its 5′end (Wang et al., 2015). There are also examples among the relatively few PPR proteins of Chlamydomonas: Mca1 binds the 5′UTR of *petA*, hinders its 5′ to 3′ exonucleolytic degradation, and, in association with Tca1, promotes its translation (Loiselay et al., 2008), while Mrl1 ensures the stability of *rbcL* mRNA (Johnson et al., 2010). The properties of Mac1 are consistent with the model that emerges from these comparisons: Mac1 could bind the 5′UTR of *psaC* and protect the downstream transcripts from exonucleolytic degradation. The combined action of 5′ and 3′ exonucleases would eventually generate a sRNA footprint. It remains an open question whether Mac1 is also involved in translation.

Mac1 Is Downregulated in Response to Iron Deficiency

The low availability of iron can be a severe limitation for the growth of photosynthetic organisms, be it in aqueous environments or on land. Both the mitochondrial respiratory chain and the photosynthetic electron chain comprise proteins that contain iron, heme, and iron-sulfur clusters as cofactors. In Chlamydomonas grown in photoheterotrophic conditions, where both respiration and photosynthesis are normally active, iron deficiency leads to the preferential allocation of the metal to mitochondrial respiration

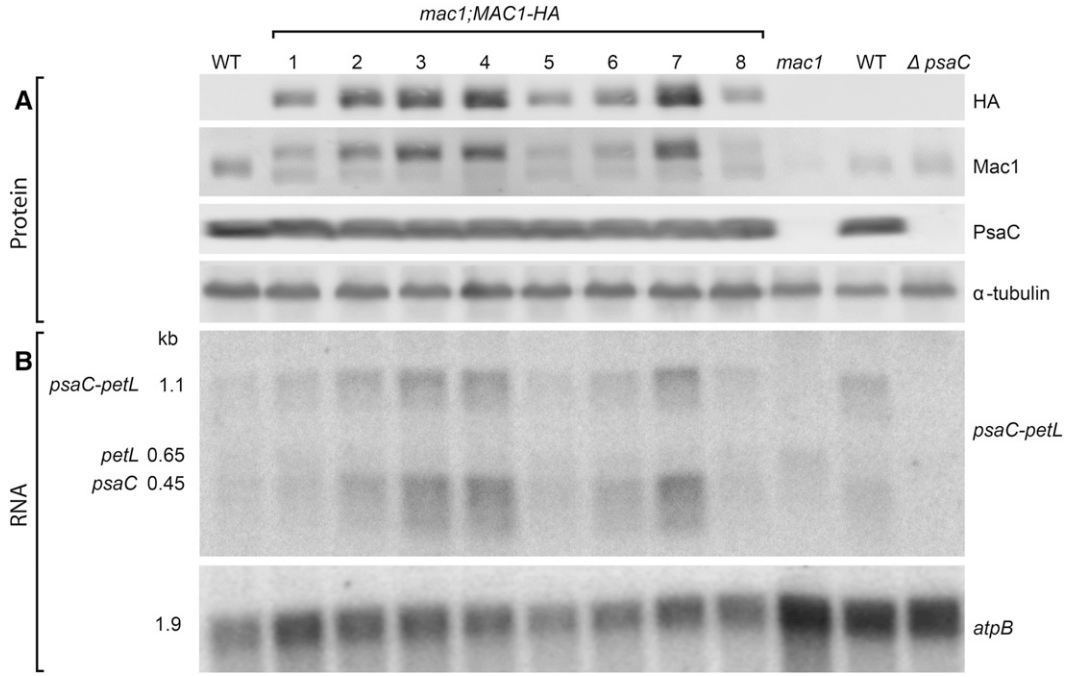

Figure 9. *psaC* RNA Accumulation Correlates with Mac1 Levels.

(A) The wild type and a series of independent *mac1* mutant lines complemented with *MAC1-HA* (*mac1;MAC1-HA* #1 to 8) were grown in iron-replete mixotrophic conditions under normal light (60 μmol m^{-2} s^{-1}). For comparison, *mac1*, the wild type, and the *ΔpsaC* mutant (with an insertion disrupting the *psaC* gene) are also shown, grown in low light (6 μmol m^{-2} s^{-1}) because PSI-deficient mutants are light sensitive. Total proteins were extracted and analyzed by SDS-PAGE and immunoblotting with the antisera indicated on the right.

(B) Total RNA was extracted from the same cultures as in **(A)** and analyzed by denaturing gel electrophoresis and blot hybridization with radiolabeled probes containing *psaC* and *petL* (upper panel) or *atpB* as a control (lower panel).

at the expense of photosynthesis (Moseley et al., 2002; Terauchi et al., 2010; Urzica et al., 2012). PSI, which contains three 4Fe4S centers, is an early target of this response: It is disconnected from its light-harvesting antenna and rapidly dismantled, like other complexes of the photosynthetic electron chain, while ATP synthase remains more stable (Moseley et al., 2002; Naumann et al., 2005). The iron that is released is bound by ferritin, which is upregulated at the level of translation (Busch et al., 2008). The response to iron deficiency also involves changes in the abundance of numerous other proteins and in particular of Taa1, which is degraded (Hohner et al., 2013; Lefebvre-Legendre et al., 2015). As previously mentioned, the latter is a nucleus-encoded protein of the OPR family that is specifically required for the stability and translation of *psaA* mRNA in the chloroplast. There is thus a clear parallel with Mac1, which controls *psaC* mRNA stability and is downregulated under iron deficiency. Hence, the response to iron limitation involves not only the degradation of the PSI complex, but also the downregulation of nucleus-encoded factors that regulate the expression of chloroplast-encoded PSI subunits. As was observed with Taa1, the decrease in Mac1 abundance is most likely regulated at the posttranscriptional level, since data from high-throughput RNA sequencing indicate that under iron limitation there is a moderate increase in *MAC1* RNA levels (Urzica et al., 2013; Phytozome v11 at https://phytozome.jgi.doe.gov/). It is interesting to compare this response to a similar response that occurs under nitrogen limitation in Chlamydomonas with the downregulation of the cytochrome b_6f complex. This latter response involves the coordinate degradation of the b_6f complex itself, of proteins that regulate the expression of its chloroplast genes, and of proteins involved in its biogenesis (Raynaud et al., 2007; Wei et al., 2014).

In response to iron deficiency, there is a correlation between the reduced accumulation of PSI subunits and of factors that govern their expression. This correlation raises the question whether the decrease of the nucleus-encoded factors has a causal role in the decrease of the chloroplast-encoded proteins. Alternatively, it cannot be excluded that the nucleus-encoded factors and the PSI subunits could be responding independently to the same nutritional cues. In other words, the question is whether Mac1 truly exerts anterograde regulation on *psaC* expression in response to iron availability. As a step toward answering this question, we sought to determine whether the amounts of Mac1 can be limiting for the accumulation of *psaC* mRNA and PsaC protein. In an allelic series of transformants expressing different levels of Mac1-HA, we observed that the accumulation of *psaC* mRNA parallels that of Mac1-HA (Figure 9). Thus, the amounts of Mac1 do seem to be limiting for the accumulation of *psaC* mRNA. However the amounts of PsaC protein were similar in all the strains of the allelic series. This may be due to the negative feedback regulation that is exerted by unassembled PsaC on translation of its own mRNA

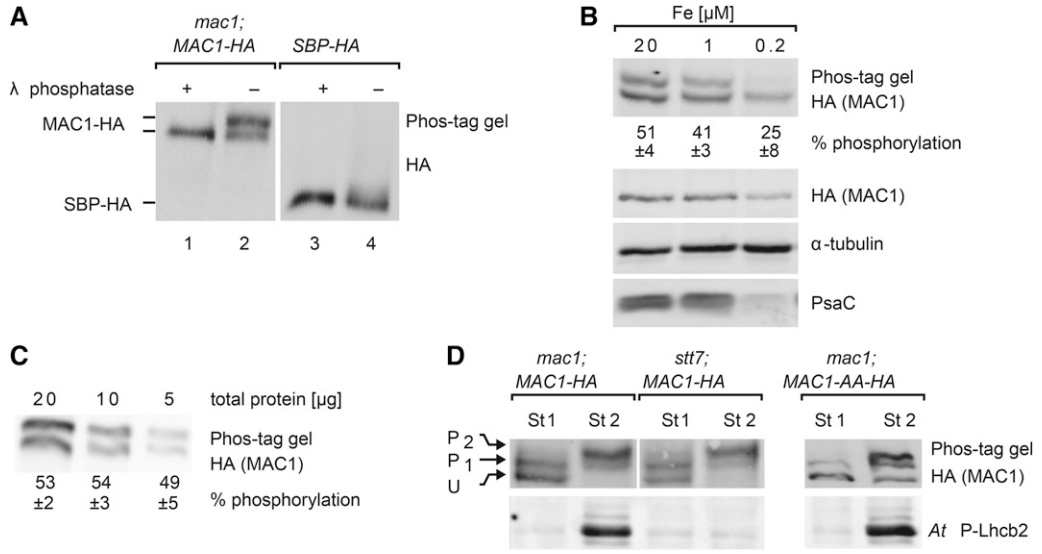

Figure 10. Mac1 Is Phosphorylated in Response to Environmental Conditions.

(A) Protein extracts of *mac1;MAC1-HA* (the *mac1* mutant complemented with an HA-epitope tagged *MAC1* gene) grown mixotrophically were analyzed by electrophoresis in polyacrylamide gels containing a gradient of Phos-tag. Prior to loading on the gels, the samples were incubated in the presence (+) or absence (−) of λ protein phosphatase as indicated at the top (lanes 1 and 2). For comparison, protein extracts of *SBP-HA* were analyzed after incubation with (+) or without (−) λ protein phosphatase (lanes 3 and 4).

(B) Top panel: Cultures of *mac1;MAC1-HA* were grown mixotrophically in the presence of different initial concentrations of Fe as described for Figure 8A. Protein extracts were analyzed by Phos-tag gel electrophoresis and immunoblotting with HA antibodies. The extent of phosphorylation (estimated as the intensity of the upper band divided by the sum of the intensities of both bands) is shown below each lane as a percentage (±SD, $n = 3$). Lower panels: The same samples were analyzed by SDS-PAGE in normal gels and immunoblotting with the antisera indicated on the right.

(C) Three different amounts of total protein from cultures with 20 μM Fe were analyzed by Phos-tag gel electrophoresis and immunoblotting with HA antibodies, and phosphorylation was calculated as in **(B)**. The estimated phosphorylation is approximately constant over the 4-fold range of total protein, indicating that in **(B)**, the decreased phosphorylation of Mac1 observed with the 0.2 μM culture is not an artifact due to the lower amount of Mac1.

(D) Cultures of *mac1;MAC1-HA*, of *stt7-7;MAC1-HA* (the *stt7-7* kinase mutant transformed with *MAC1-HA*), or of *mac1;MAC1-AA-HA* (with serines 137 and 139 changed to alanines) were treated under conditions that favor oxidation of the plastoquinone pool (state 1, 10 μM DCMU in the light; lanes 1, 3, and 5) or its reduction (state 2, anaerobiosis in the dark; lanes 2, 4, and 6). Protein extracts were analyzed by Phos-tag gel electrophoresis and immunoblotting with HA antibodies (upper panel) or by SDS-PAGE in normal gels and immunoblotting with phospho-specific antiserum against phosphorylated Lhcb2 of Arabidopsis (*At* P-Lhcb2; lower panel). That the conditions were effective in promoting state 1 or state 2 is shown by the widely different levels of phosphorylation of LHCII. The exposure shown for *stt7-7;MAC1-HA* is longer than for *mac1;MAC1-HA* because of different levels of Mac1-HA expression in the two strains.

(Control by Epistasy of Synthesis [CES]) (Wostrikoff et al., 2004). In the Mac1-HA overexpressors, any excess of PsaC that cannot be assembled with PsaA and PsaB is expected to inhibit its own translation and eventually to be degraded (Choquet and Vallon, 2000). Thus, the biosynthesis of PsaC would not be affected by increases in the amount of *psaC* mRNA above what actually is required for translation (Hosler et al., 1989).

Mac1 Is Phosphorylated to Different Extents Depending on Growth Conditions

Protein phosphorylation is a prevalent posttranslational modification that plays an important role in the regulation of numerous processes in biology. Hundreds of phosphoproteins that are known or predicted to localize to the chloroplast have been identified in large-scale proteomic studies, both in Chlamydomonas and in vascular plants (Lohrig et al., 2009; Reiland et al., 2009; Wang et al., 2014). In plastids, protein phosphorylation plays regulatory roles in photosynthesis, gene expression, and metabolism (Baginsky and Gruissem, 2004). Thylakoid proteins such as LHCII and PSII are some of the most abundant chloroplast phosphoproteins. The phosphorylation of LHCII, which is largely dependent on the protein kinase Stt7 in Chlamydomonas and STN7 in plants, plays a role in a regulatory response to changing light quality and to metabolic demands of the cell known as state transition (Depege et al., 2003). Reversible phosphorylation regulates the dynamic allocation of LHCII to PSI or PSII. The phosphorylation of the PSII core subunits by the protein kinase STN8, a paralog of STN7, plays a role in the organization of the thylakoid membranes and in the repair cycle of photodamaged PSII in Arabidopsis (Bonardi et al., 2005; Tikkanen et al., 2008; Fristedt et al., 2009).

Focusing on the role of protein phosphorylation for gene expression in the chloroplast of vascular plants, there is evidence for regulation both at the level of transcription and at post-transcriptional steps. The chloroplast sensor kinase, which is related to bacterial two-component sensor kinases, is reported to play a role in the regulation of plastid transcription as a function of

photosynthetic activity (Puthiyaveetil et al., 2008). The chloroplast casein kinase 2 (cpCK2), also known as Plastid Transcription Kinase (PTK) because of its association with RNA polymerase complexes, is involved in the regulated phosphorylation of sigma factors that play a role in promoter recognition (Schweer et al., 2010). At the posttranscriptional level, chloroplast ribonucleoproteins are phosphorylated by cpCK2, and in the case of 28RNP, phosphorylation can influence RNA binding in vitro (Kanekatsu et al., 1995; Lisitsky and Schuster, 1995). Phosphorylation by cpCK2/PTK also regulates the activity of the chloroplast endoribonuclease p54 in vitro (Liere and Link, 1997).The targets of cpPK2 are not limited to proteins involved in gene expression and, for example, also include the β-subunit of ATP-synthase in the thylakoid membrane (Kanekatsu et al., 1998). The fact that the kinase STN7 is itself a phosphoprotein and the presence in the plastid of numerous other protein kinases are suggestive of a complex regulatory phosphorylation network in the chloroplast of vascular plants (Baginsky and Gruissem, 2004; Reiland et al., 2011; Bayer et al., 2012).

Little is known about the phosphorylation of proteins involved in chloroplast gene expression in Chlamydomonas. Using electrophoresis in Phos-tag gradient gels and immunoblotting, we revealed that Mac1 is phosphorylated (Figure 10). Two phosphorylated forms of Mac1-HA were resolved with this gel system (P_1 and P_2), which could represent mono- and diphosphorylated Mac1-HA or two different forms with different degrees of multiple phosphorylation. A first indication that phosphorylation of Mac1 changes with the environmental conditions came with the observation that under conditions of iron deficiency, there was a decrease in the proportion of the phosphorylated form, concomitant with a reduction in the total amount of Mac1-HA. This raises the interesting but open question of whether phosphorylation has an influence on the proteolytic degradation of Mac1. A second indication came with Chlamydomonas cells that were incubated under anaerobiosis in the dark, a condition that induces state 2, with the reduction of plastoquinone and the consequent activation of Stt7 (Wollman and Delepelaire, 1984). In this condition, a strong phosphorylation of Mac1-HA was observed, with the appearance of the slower migrating form (P_2). Conversely, in a condition that induces the oxidation of the plastoquinone pool and state 1, incubation in dim light in the presence of DCMU, phosphorylation of Mac1 was less extensive. However, in the *stt7-7* mutant background, the strong phosphorylation with the presence of two phosphorylated forms of Mac1-HA was still observed in state 2 conditions. Hence, the kinase, or possibly the kinases, responsible for Mac1 phosphorylation remain elusive. A possible candidate could be Stl1, the paralog of Stt7 in Chlamydomonas, for which no mutant has yet been described. The physiological significance of Mac1 phosphorylation will need to be investigated in future experiments, in particular to determine whether phosphorylation might affect its RNA binding activity or its proteolytic turnover.

Among the proteins involved in posttranscriptional steps of chloroplast gene expression, two general groups can be distinguished. One includes the proteins that bind a large set of chloroplast RNAs with little gene specificity, such as the cpRNP proteins that intervene at multiples steps of gene expression (Kupsch et al., 2012). The other consists of the proteins that bind to a restricted subset of plastid transcripts or to a single one and have more specific roles. As discussed above, it is known that some of the proteins of the former group are phosphorylated. Our current work establishes that a member of the latter group, namely, Mac1, is also subject to phosphorylation. This observation opens many new questions about the posttranscriptional regulation of chloroplast gene expression.

METHODS

Strains and Growth Conditions

Cells were grown in Tris acetate phosphate (TAP) or high salt minimal (HSM) media (Kropat et al., 2011) in the dark, under low light (6 μmol m^{-2} s^{-1}) or normal light (60 μmol m^{-2} s^{-1}) from fluorescent tubes. The original mutant isolate was backcrossed three times to a wild-type strain (137c), and a spore from the last cross was used in this work as *mac1* (mating type minus).

For growth under iron limitation, the glassware was treated with sterile 10 mM EDTA for 15 min and rinsed three times with sterile MilliQ water before use. Precultures were grown for at least 10 doublings under normal light in TAP medium, collected by centrifugation, and washed three times in TAP without Fe. Cells were then diluted to 2×10^5 cells/mL, supplemented with 0.2, 1.0, or 20 μM $FeCl_3$, and grown for 10 doublings with intermediate dilutions to maintain the concentration below 2×10^6.

The state transitions were obtained with cells grown in TAP and normal light. The cells were shifted to HSM medium with three steps of centrifugation and washing, and incubated with shaking in the dark for 2 h. They were then collected by centrifugation and resuspended in HSM medium to a concentration of 2×10^7 cells/mL and split in two aliquots. State 1 was induced during 1 h and 30 min by gentle agitation in low light with 10 μM DCMU. State 2 was obtained by incubating 1 h and 30 min in the dark in a sealed 2-mL syringe without air bubbles on a rotating wheel.

Identification of *MAC1*

The mutant was generated by random insertional mutagenesis of an *aphVIII* cassette into the wild-type line *jex4* and screened for aberrant chlorophyll fluorescence kinetics as described previously (Houille-Vernes et al., 2011). The mutation was identified by inverse PCR as follows. Total DNA from the mutant was extracted with the DNeasy plant mini kit (Qiagen), and 100 ng was digested with BstU1 for 5 h. The enzyme was inactivated by heat treatment and the DNA was purified through phenol-chloroform extraction followed by ethanol precipitation. The DNA from the pellet was ligated with T4 ligase overnight at 16°C in a volume of 70 μL, and 5 μL aliquots were used as templates for nested PCR. The first PCR was with primers IP2 and IP3 (Supplemental Table 1) in a final volume of 25 μL (45 s at 95°C, 45 s at 55°C, and 2 min at 72°C, 35 cycles). A 1-μL aliquot was then used for a second round with primers IP1 and IP4. Sequencing of the fragment and a BLAST search of the *Chlamydomonas reinhardtii* genome showed that the insertion mapped to exon 2 of Cre09.g389615 (g9646.t1) in version 11 of the Phytozome database (https://phytozome.jgi.doe.gov/pz/portal.html). This locus is included in the BAC clone 23A16 (Lefebvre and Silflow, 1999).

DNA Constructs

The plasmids MAC1_gen3 and MAC1-HA were obtained as illustrated in Supplemental Figure 8A. A 4-kb *Bsp*HI fragment containing the 3′ flank and most of the coding sequence was cloned in the TOPO vector pCR2.1 from a digest of BAC 23A16. This plasmid (Mac1-genomic-TOPO) was then extended with a PCR fragment (prepared with primers IF-EcorV-Sbf1-for and IF-Rev; Supplemental Table 1) containing the beginning of the gene

and the 5′ flanking promoter region using Gibson assembly (Gibson et al., 2009). The final construct (MAC1-gen3) contains ~1 kb upstream of the predicted coding sequence and 1 kb downstream. To insert the triple HA (hemagglutinin) epitope tag at the C terminus of the coding sequence, a synthetic *Bsm*I-*Bsi*WI fragment (obtained from Biomatik) was cloned into the corresponding sites of Mac1-genomic-TOPO. The beginning of the gene and the 5′ flanking promoter region were then added as above. A transformant expressing the HA-tagged Mac1 at a level similar to the wild type (#6 in Figure 9) was selected and designated in this work as *mac1; MAC1-HA*. The *MAC1-AA-HA* mutant plasmid was derived from *MAC1-HA* by replacing the *Bst*EII-*Nru*I fragment with two overlapping PCR fragments (obtained with oligonucleotides mut5′macfor with S137A_S139A_R and S137A_S139A_F with mut-mac-rev, respectively, and *MAC1-HA* as template; Supplemental Table 1) using Gibson assembly.

The *psaC:lucCP:rbcL* reporter construct was obtained by replacing the *acrV* gene in the atpB-INT-psaA:acrV vector (Michelet et al., 2011) with the *lucCP* gene (Matsuo et al., 2006) using *Nco*I and *Sph*I. The *psaC* 5′ flank (promoter and 5′UTR) was amplified by PCR with primers (psaCprom3′BspH1 and psaCprom5; Supplemental Table 1), subcloned in the Topo vector pCR 2.1 and inserted as a *Xba*I-*Bsp*HI fragment in a *Xba*I-*Nco*I digest of the vector.

The transformation vector containing *MAC1-HA* used for transformation of *stt7-7* was obtained by inserting the *aph 7"* hygromycin resistance cassette (Berthold et al., 2002) as a PCR fragment (obtained with primers MacHA_hyg_F and MacHA_hyg_R; Supplemental Table 1) at the *Xba*I site of MAC1_gen3 using Gibson assembly. The final construct was transformed using a helium gene gun into the *stt7-7* mutant (Depege et al., 2003) with selection on 20 μg/mL hygromycin (Calbiochem). A transformant expressing Mac1-HA was identified by immunoblotting.

Transformation

Nuclear transformation by electroporation was modified from Shimogawara et al. (1998). A volume of 300 μL of cells suspended at 10^8 cell/mL in either HSM + 40 mM sucrose or TAP + 40 mM sucrose (for selection for photoautotrophy or for antibiotic resistance, respectively) were incubated with 2 μg DNA at 16°C for 20 min, and then 250 μL of the mix was transferred to a 4-mm-gap electroporation cuvette and pulsed at 750 V (C = 50 μF). After 2 min incubation at room temperature, the cuvettes were transferred to 16°C for 20 min. The cell suspension was plated with 1 mL of HSM containing 25% starch (for photoautotrophy) or transferred to 50 mL TAP (without sucrose) overnight in low light and collected by centrifugation prior to plating with TAP starch (for antibiotic resistance).

Chloroplast transformation was described previously (Vaistij et al., 2000b).

Mac1 Antiserum

The Mac1 antiserum was raised in a rabbit with the C-terminal region of Mac1 prepared as follows. The *MAC1* cDNA was amplified by PCR from a cDNA library (with the primers mac1-half-for and rev-xho; Supplemental Table 1), cloned in TOPO vector pCR2.1, and transferred to pET28a (Novagen) (Supplemental Figure 8B). This vector (pET28Mac1cter) was used to transform *Escherichia coli* BL21 cells and the protein (tagged with six histidines encoded by the vector) was purified using Ni-NTA affinity chromatography and imidazole elution, followed by gel filtration on Sephadex S200. The rabbit serum was used at 1/5000 dilution for immunoblots.

Immunoblotting

Cell pellets were resuspended in lysis buffer containing 50 mM Tris, pH 6.8, 5% SDS, 10 mM EDTA, and 1× Protease inhibitor cocktail (Sigma-Aldrich). Samples (25 μg each) were supplemented with 0.2 volumes of sample buffer (10% SDS [w/v], 250 mM Tris, pH 6.8, 50% glycerol [v/v], 500 mM DTT, and bromophenol blue) and heated at 55°C for 15 min. Proteins were separated by SDS-PAGE on 15 or 7% acrylamide gels and transferred to nitrocellulose membranes. The total protein on the membrane was visualized by amido black staining, and the membrane was blocked in Tris-buffered saline Tween (TBST; 20 mM Tris, pH 7.5, 150 mM NaCl, and 1% [v/v] Tween 20) supplemented with 5% (w/v) nonfat milk for 1 h. The membrane was incubated with primary antibody in TBST and 1% milk. The primary antisera (and their sources) were as follows: monoclonal anti-HA (Covance; MMS-101R), antiphospho-Lhcb2 (Agrisera; AS13-2705), antiRpl4 (gift of W. Zerges), anti-PsaA (Redding et al., 1998), anti-Cyt_f (gift of F.-A. Wollman), anti-PsaC, anti-D1 (gifts of J.-D. Rochaix), anti-Rpl37, and anti-Rps12 (Ramundo et al., 2013). The membranes were washed three times for 10 min and then incubated for 2 h with horseradish peroxidase-conjugated secondary antibody (Promega). After three washes, the detection was performed by enhanced chemiluminescence and imaging with the GE LAS4000 system (General Electric).

RNA Hybridization

Cells were grown in the indicated conditions until they reached 2×10^6 cells/mL. They were then centrifuged 2000*g* for 5 min, aliquoted as pellets of 2×10^7 cells, frozen in liquid nitrogen, and kept at −80°C until their use. RNA from the frozen pellet was extracted using the RNeasy Kit (Qiagen) and analyzed by 1.2% agarose MOPS formaldehyde gel electrophoresis and capillary transfer to nylon membranes Hybond N^+ (Amersham) (Sambrook et al., 1989). The hybridization was done in Church and Gilbert hybridization buffer with ^{32}P-labeled probes as described (Rio et al., 2011) The probes were obtained by PCR with the oligonucleotides listed in Supplemental Table 1 and total genomic DNA as template, except for the *psaA exon1* probe, which was a 280-bp *Hind*III fragment.

Probes were stripped in 0.1% SDS, 1 mM phosphate buffer, pH 7, and 1 mM EDTA at 98°C for 5 min, and the membranes were checked for residual signal by phosphor imaging. The RNA gel blots presented in Figures 1, 2, 8, and 9 and the run-on transcription assay in Figure 4 were all obtained using one membrane for each that was repeatedly stripped, checked for absence of residual signal, and reprobed.

Immunofluorescence

The protocol for immunofluorescence was described previously (Lefebvre-Legendre et al., 2015). The HA signal was revealed with goat anti-mouse antibodies coupled to Alexafluor 647 (excitation, 647 nm; emission, 660 to 750 nm). The other antibodies were revealed with goat anti-rabbit antibodies coupled to Alexafluor 546 (excitation, 546 nm; emission, 560 to 600 nm).

Cell Fractionation and Sucrose Gradient Sedimentation Analysis

Cell fractionation was described previously (Lefebvre-Legendre et al., 2015), using the protocol of Percoll gradient chloroplast isolation from Rivier et al. (2001).

For sucrose gradient sedimentation analysis, cells from a 250-mL culture of *mac1;MAC1-HA* (2.10^6 cells mL^{-1}) were collected and resuspended in 1.1 mL HKM buffer (20 mM HEPES, pH 7.2, 50 mM KCl, and 10 mM $MgCl_2$) supplemented with protease inhibitor cocktail (Roche EDTA-free tabs). The sample was frozen as 100 μL drops in liquid nitrogen and ground in a 50-mL compartment of a MM400 beadbeater (Retsch) for 2 min at 30 cycles s^{-1}.The powder was then collected, melted on ice, and centrifuged for 20 min at 15,000*g*. Aliquots of the supernatant (800 μL) were mixed with 100 μL RNase buffer (100 mM Tris, pH 7.5, and 10 mM sodium acetate) with or without (mock treatment) 10 μg mL^{-1} RNaseA and incubated for 10 min at 22°C. The samples were loaded on 10-mL sucrose gradients (HKM buffer, 5 to 45%

sucrose) as described previously (Lefebvre-Legendre et al., 2015). Twenty fractions (500 μL) were collected from the bottom. Aliquots (150 μL) were precipitated (Wessel and Flugge, 1984) by sequential addition with thorough mixing of 600 μL methanol, 150 μL chloroform, and 450 μL water, followed by centrifugation for 5 min at 14,000*g*. The clear upper aqueous layer was discarded and the bottom phase with the white protein interface was washed with 1 mL 50% (v/v) methanol, vortexed, and centrifuged again. The bottom phase with the protein interface was supplemented with 650 μL methanol, inverted three times, and centrifuged for 5 min. The pellets were dried and resuspended in 100 μL buffer (100 mM Tris-HCl, pH 7, 3% SDS [w/v], 10% glycerol [v/v], and 80 mM DTT), treated 10 min at 55°C, and finally analyzed by SDS-PAGE (7% acrylamide) and immunoblotting with anti-HA monoclonal antibody (Covance) or anti-Rubisco (gift of Jean-David Rochaix, University of Geneva).

Run-on Transcription Assay

The protocol was modified from Klinkert et al. (2005). A total of 10^8 cells in early exponential phase were harvested by centrifugation and washed with resuspension buffer (10 mM HEPES, pH 7.5, 150 mM KCl, 250 mM sucrose, 1 mM EDTA, and 0.1 mM PMSF). The pellet was adjusted to 100 μL with the same buffer and frozen in liquid nitrogen. Then, 40 μL 4× run-on buffer (100 mM HEPES, pH 7.5, 1 M sucrose, 120 mM $MgCl_2$, 30 mM DTT, and 100 mM NaF) was mixed with 5 μL each of 10 mM rATP, rGTP, and rCTP, 5 μL RNasin (Promega), 20 μL ^{32}P-rUTP (200 μCi, 5 μM final), and 80 μL of cell pellet (defrosted in a water bath at 20°C).The reaction mixture was incubated at 26°C for 5 or 15 min. Total RNA was immediately extracted with TRI Reagent (Sigma-Aldrich), precipitated with isopropanol, and resuspended in TE (10 mM Tris and 1 mM EDTA, pH 8) prior to separation on a Sephadex G50 column. The RNA fractions were then used for hybridization. The membrane was prepared by spotting DNA probes prepared by PCR (see above) onto a Hybond N^+ nylon membrane (Amersham). The membrane was then dried and cross-linked using the automatic mode of a UV cross-linker (Stratalinker). Hybridization of the labeled RNA probes to the membrane was performed as described above for RNA gel blots.

sRNA

Published Chlamydomonas sRNA sequencing data (Ibrahim et al., 2010) were mapped to the chloroplast genome (NC_005353) as described (Loizeau et al., 2014). Read coverage within the *psaC* 5′UTR and the 5′ end of the *psaC* coding sequence were visualized using the Integrated Genomics Viewer (Figure 5A). For experimental verification of identified sRNAs, total RNA from dark-grown cells was extracted with TRI Reagent (Sigma-Aldrich). sRNA enrichment was performed as described (Loizeau et al., 2014). Enriched sRNAs (10 μg) were separated by denaturing PAGE, blotted, and hybridized to an end-labeled DNA oligonucleotide named *psaC*4as (Supplemental Table 1) situated antisense to the putative sRNA within the 5′UTR of *psaC*.

Luciferase Assay

The different strains were grown in TAP medium under normal light to 2 × 10^6 cells/mL. For transformants of *psaB:lucCP*, 50-μL aliquots of each culture were placed in the wells of a white-walled microtiter plate sitting on dry ice. Cultures of *psaC:lucCP* were concentrated 10-fold by centrifugation before freezing. Frozen plates were kept at −20°C prior to the measurement. For the assay, 100 μL luciferase reagent (50 mM potassium phosphate buffer, pH 7, 150 mM NaCl, 1× Protease inhibitor cocktail [Sigma-Aldrich], 2.5 mM ATP, 2.5 mM $MgCl_2$, and 4 mM luciferin [Promega]) was added to the frozen sample and the luminescence emission kinetics monitored at 28°C for 30 min using a Synergy 2 plate reader (Biotek). The maximum luminescence was used for the quantification.

Mac1 Purification and RNA Binding Assays

The sequence encoding MAC1 lacking the transit peptide was amplified by PCR with the oligonucleotides cdna_pet_ inf_for and cdna_pet_inf_rev (Supplemental Table 1). The PCR fragment (2695 bp) was cloned between the *Nco*I and *Xho*I sites of pET28a using Gibson assembly. The construct was freshly transformed into *E. coli* BL21(DE3) cells for each purification. The bacteria were cultivated in 2 liters Luria-Bertani medium containing 50 μg mL^{-1} kanamycin until the culture reached an absorbance of 0.25 at 600 nm. Cultures were transferred to ice for 15 min, and IPTG was added to 100 μM and ethanol to 1% (v/v). After 15 more minutes, the culture was transferred to an incubator at 18°C and agitated for 20 h. Cells were harvested by centrifugation and the pellet was used immediately. The cells were resuspended on ice in 25 mL lysis buffer (50 mM HEPES, pH 7.7, 750 mM NaCl, 5 mM $MgCl_2$, and 4 mM DTT) containing proteinase inhibitors (Roche EDTA-free tabs), and lysed by three passages in the EmulsiFlex C-3 at 20,000 p.s.i. The resulting extract was centrifuged 30 min at 12,000*g* and the supernatant was loaded on a 1-mL Ni-NTA column, washed with lysis buffer supplemented with 30 mM imidazole, and eluted with 5 mL of 25 mM HEPES, pH 7.7, 750 mM NaCl, 5 mM $MgCl_2$, 4 mM DTT, and 300 mM imidazole. The extract was then directly injected onto the size exclusion column (HiLoad Sephadex 200 16/60, AKTA system; GE Healthcare) and eluted in column buffer (50 mM Tris, pH 7.7, 250 mM NaCl, 4 mM DTT, and 10% [v/v] glycerol) at 0.6 mL·min^{-1}.

A vector for the preparation of the RNA probe was obtained by cloning the following sequence in the TOPO pCR2.1 (Invitrogen) vector: TAATACGACTCACTATAGGGAGA**AAGTCGATTCTCAATCTTCTTTTTGATATGGAGATGACATATTTAGCACAA***TCGAT*. The T7 promoter is underlined, the 5′ part of the *psaC* UTR is highlighted in bold, and a *Cla*I site is shown in italics. The vector was digested with *Apa*I (in the vector) and *Cla*I (shown above in italics), leading to a fragment of 139 bp, which was purified by agarose gel electrophoresis and transcribed in vitro with T7 RNA polymerase (Promega) for 2 h at 30°C in a 20-μL reaction mixture containing: 4 μL transcription buffer (Promega), 1 μL 1 mM rUTP, 1 μL each 10 mM stocks of the three other nucleotide triphosphates, 3 μL ^{32}P-rUTP at 10 mCi mL^{-1} and 3000 Ci $mmol^{-1}$, 1 μL RNase-in (Promega), 1 μL 20 mM DTT, 1 μL T7 polymerase, and 200 ng probe. This produced a 62-nucleotide RNA containing the first 51 nucleotides of the *psaC* 5′UTR. After treatment with RQ1 DNase (Promega) for 30 min, the labeled RNA was separated from the free nucleotides on a size-exclusion column (Sephadex G25 fine).

The binding conditions for electrophoretic mobility shift assay were previously described (Williams-Carrier et al., 2008). The buffer used was the column buffer supplemented with 0.04 mg/mL BSA (Applichem), 0.5 mg/mL Heparin (Sigma-Aldrich), and 4000 cpm radiolabeled RNA probe (40 pM) in a final volume of 20 μL. The K_d was determined as the Mac1 concentration at which half of the probe was bound by the protein, which is a valid approximation when the protein is in large excess over the RNA in the assay (30 to 100 nM versus 40 pM).

Phos-Tag Gel Electrophoresis

Chlamydomonas culture (10 mL) was added to 40 mL cold acetone and precipitated overnight at −20°C. After centrifugation at 3000*g* for 20 min, the pellet was resuspended in 200 μL sample buffer (50 mM HEPES, pH 7.8, 200 mM NaCl, 1× complete protease inhibitor [Roche ETDA-free], and 0.5% Triton X-100). The suspension was transferred to a 1.5-mL microtube, 500 μL acid-washed glass beads (0.4 to 0.6 mm) were added, and the samples were homogenized two times for 15 s in a Silamat shaker. The mixture was then centrifuged at 20,000*g* for 20 min, and the supernatant was transferred to a new tube. For dephosphorylation, an aliquot containing 25 μg protein was brought to 50 μL in lambda protein phosphatase reaction mix following the instructions of the manufacturer (New England Biolabs) and treated for 1 h at 30°C.

For Phos-tag [Wako; *N*-(5-(2-aminoethylcarbamoyl)pyridin-2-ylmetyl)-*N*,*N*′,*N*′-tris(pyridin-2-yl-methyl)-1,3-diaminopropan-2-ol] gel electrophoresis (Kinoshita and Kinoshita-Kikuta, 2011), a modified protocol was used that improves the migration, separation, and electrophoretic transfer of Mac1 to the nitrocellulose membrane (Longoni et al., 2015). The gel was prepared in 0.35 M Bis-Tris buffer system, pH 6.8, and contained a Phos-tag gradient prepared as described in Supplemental Figure 7.

Phylogenetic Analysis

The phylogenetic tree was constructed with the MEGA6 software (Tamura et al., 2013), using ClustalW (with default parameters) to derive the protein sequence alignment, which was manually curated to remove divergent N-terminal sequences (Supplemental Data Set 1). The phylogenetic reconstruction used the maximum likelihood method (with default parameters) and 1000 bootstrap replicates.

Accession Numbers

Sequence data from this article can be found in public databases under the following accession numbers: *MAC1*, Cre09.g389615 (g9646.t1) (Phytozome v11); Mbb1, XP_001696751.1 (GenBank); HCF107, NP_188329 (GenBank).

Supplemental Data

Supplemental Figure 1. Identification of the *MAC1* gene.

Supplemental Figure 2. Complementation of the *mac1* mutant.

Supplemental Figure 3. Phylogenetic analysis of Mac1.

Supplemental Figure 4. Localization of Mac1-HA by immunofluorescence confocal microscopy.

Supplemental Figure 5. Small RNA footprints in the 5′UTR of *psaC.*

Supplemental Figure 6. Quantification of PsaC, Mac1, and *psaC* mRNA under iron limitation.

Supplemental Figure 7. Phos-tag gel electrophoresis.

Supplemental Figure 8. Construction of DNA clones and vectors.

Supplemental Table 1. Oligonucleotides used in this work.

Supplemental Data Set 1. Text file of the alignment used for the phylogenetic analysis in Supplemental Figure 3.

ACKNOWLEDGMENTS

This work was supported by the University of Geneva, the Institute of Genetics and Genomics of Geneva (iGE3), the Swiss National Fund (Grants 31003A_146300 and 3100A0-117712), the European Union's Seventh Framework Programme for Research, Technological Development, and Demonstration (FP7 KBBE 2009-3 Sunbiopath, GA 245070), the French Centre National de la Recherche Scientifique, the Université Pierre et Marie Curie Paris 06, the Fondation Pierre Gilles de Gennes pour la Recherche, and the Deutsche Forschungsgemeinschaft (SCHM 1698/5-1). We thank Jean Alric for contributing to the genetic screen of Chlamydomonas photosynthesis mutants, Geoffrey Fucile for help with the phylogenetic analysis, Gongwei Wang for help with IGV analyses, and Christoph Bauer, Jérôme Bosset, and Sylvain Loubéry for support with immunofluorescence confocal microscopy. We also acknowledge Yuichiro Takahashi for the *ΔpsaC* mutant, and Jean-David Rochaix, Francis-André Wollman, and Catherine de Vitry for their scientific advice.

AUTHOR CONTRIBUTIONS

D.D., Y.Q., P.L., L.L.-L., X.J., C.S.-L., and M.G.-C. designed the research. D.D., Y.Q., P.L., L.L.-L., and X.J. performed research. D.D. and M.G.-C. wrote the article.

Received August 17, 2015; revised April 7, 2016; accepted April 25, 2016; published April 25, 2016.

REFERENCES

Baginsky, S., and Gruissem, W. (2004). Chloroplast proteomics: potentials and challenges. J. Exp. Bot. **55:** 1213–1220.

Bai, Y., Auperin, T.C., Chou, C.Y., Chang, G.G., Manley, J.L., and Tong, L. (2007). Crystal structure of murine CstF-77: dimeric association and implications for polyadenylation of mRNA precursors. Mol. Cell **25:** 863–875.

Barkan, A. (2011). Expression of plastid genes: organelle-specific elaborations on a prokaryotic scaffold. Plant Physiol. **155:** 1520–1532.

Barkan, A., Rojas, M., Fujii, S., Yap, A., Chong, Y.S., Bond, C.S., and Small, I. (2012). A combinatorial amino acid code for RNA recognition by pentatricopeptide repeat proteins. PLoS Genet. **8:** e1002910.

Barkan, A., and Small, I. (2014). Pentatricopeptide repeat proteins in plants. Annu. Rev. Plant Biol. **65:** 415–442.

Bayer, R.G., Stael, S., Rocha, A.G., Mair, A., Vothknecht, U.C., and Teige, M. (2012). Chloroplast-localized protein kinases: a step forward towards a complete inventory. J. Exp. Bot. **63:** 1713–1723.

Berthold, P., Schmitt, R., and Mages, W. (2002). An engineered *Streptomyces hygroscopicus* aph 7" gene mediates dominant resistance against hygromycin B in *Chlamydomonas reinhardtii*. Protist **153:** 401–412.

Bonardi, V., Pesaresi, P., Becker, T., Schleiff, E., Wagner, R., Pfannschmidt, T., Jahns, P., and Leister, D. (2005). Photosystem II core phosphorylation and photosynthetic acclimation require two different protein kinases. Nature **437:** 1179–1182.

Boudreau, E., Takahashi, Y., Lemieux, C., Turmel, M., and Rochaix, J.D. (1997). The chloroplast ycf3 and ycf4 open reading frames of *Chlamydomonas reinhardtii* are required for the accumulation of the photosystem I complex. EMBO J. **16:** 6095–6104.

Boulouis, A., Raynaud, C., Bujaldon, S., Aznar, A., Wollman, F.A., and Choquet, Y. (2011). The nucleus-encoded trans-acting factor MCA1 plays a critical role in the regulation of cytochrome f synthesis in Chlamydomonas chloroplasts. Plant Cell **23:** 333–349.

Busch, A., Rimbauld, B., Naumann, B., Rensch, S., and Hippler, M. (2008). Ferritin is required for rapid remodeling of the photosynthetic apparatus and minimizes photo-oxidative stress in response to iron availability in *Chlamydomonas reinhardtii*. Plant J. **55:** 201–211.

Choquet, Y., Goldschmidt-Clermont, M., Girard-Bascou, J., Kück, U., Bennoun, P., and Rochaix, J.D. (1988). Mutant phenotypes support a trans-splicing mechanism for the expression of the tripartite psaA gene in the *C. reinhardtii* chloroplast. Cell **52:** 903–913.

Choquet, Y., and Vallon, O. (2000). Synthesis, assembly and degradation of thylakoid membrane proteins. Biochimie **82:** 615–634.

Dauvillée, D., Stampacchia, O., Girard-Bascou, J., and Rochaix, J.D. (2003). Tab2 is a novel conserved RNA binding protein required for translation of the chloroplast psaB mRNA. EMBO J. **22:** 6378–6388.

Depège, N., Bellafiore, S., and Rochaix, J.D. (2003). Role of chloroplast protein kinase Stt7 in LHCII phosphorylation and state transition in Chlamydomonas. Science **299:** 1572–1575.

Felder, S., Meierhoff, K., Sane, A.P., Meurer, J., Driemel, C., Plücken, H., Klaff, P., Stein, B., Bechtold, N., and Westhoff, P. (2001). The nucleus-encoded HCF107 gene of Arabidopsis provides a link between intercistronic RNA processing and the accumulation of translation-competent psbH transcripts in chloroplasts. Plant Cell **13:** 2127–2141.

Fisk, D.G., Walker, M.B., and Barkan, A. (1999). Molecular cloning of the maize gene crp1 reveals similarity between regulators of mitochondrial and chloroplast gene expression. EMBO J. **18:** 2621–2630.

Fristedt, R., Willig, A., Granath, P., Crèvecoeur, M., Rochaix, J.D., and Vener, A.V. (2009). Phosphorylation of photosystem II controls functional macroscopic folding of photosynthetic membranes in Arabidopsis. Plant Cell **21:** 3950–3964.

Gibson, D.G., Young, L., Chuang, R.Y., Venter, J.C., Hutchison III, C.A., and Smith, H.O. (2009). Enzymatic assembly of DNA molecules up to several hundred kilobases. Nat. Methods **6:** 343–345.

Glaesener, A.G., Merchant, S.S., and Blaby-Haas, C.E. (2013). Iron economy in *Chlamydomonas reinhardtii*. Front. Plant Sci. **4:** 337.

Goldschmidt-Clermont, M., Choquet, Y., Girard-Bascou, J., Michel, F., Schirmer-Rahire, M., and Rochaix, J.D. (1991). A small chloroplast RNA may be required for trans-splicing in *Chlamydomonas reinhardtii*. Cell **65:** 135–143.

Goldschmidt-Clermont, M., Girard-Bascou, J., Choquet, Y., and Rochaix, J.D. (1990). Trans-splicing mutants of *Chlamydomonas reinhardtii*. Mol. Gen. Genet. **223:** 417–425.

Gray, M.W., Lukes, J., Archibald, J.M., Keeling, P.J., and Doolittle, W.F. (2010). Cell biology. Irremediable complexity? Science **330:** 920–921.

Guertin, M., and Bellemare, G. (1979). Synthesis of chloroplast ribonucleic acid in *Chlamydomonas reinhardtii* toluene-treated cells. Eur. J. Biochem. **96:** 125–129.

Hammani, K., Bonnard, G., Bouchoucha, A., Gobert, A., Pinker, F., Salinas, T., and Giegé, P. (2014). Helical repeats modular proteins are major players for organelle gene expression. Biochimie **100:** 141–150.

Hammani, K., Cook, W.B., and Barkan, A. (2012). RNA binding and RNA remodeling activities of the half-a-tetratricopeptide (HAT) protein HCF107 underlie its effects on gene expression. Proc. Natl. Acad. Sci. USA **109:** 5651–5656.

Höhner, R., Barth, J., Magneschi, L., Jaeger, D., Niehues, A., Bald, T., Grossman, A., Fufezan, C., and Hippler, M. (2013). The metabolic status drives acclimation of iron deficiency responses in *Chlamydomonas reinhardtii* as revealed by proteomics based hierarchical clustering and reverse genetics. Mol. Cell. Proteomics **12:** 2774–2790.

Hosler, J.P., Wurtz, E.A., Harris, E.H., Gillham, N.W., and Boynton, J.E. (1989). Relationship between gene dosage and gene expression in the chloroplast of *Chlamydomonas reinhardtii*. Plant Physiol. **91:** 648–655.

Houille-Vernes, L., Rappaport, F., Wollman, F.A., Alric, J., and Johnson, X. (2011). Plastid terminal oxidase 2 (PTOX2) is the major oxidase involved in chlororespiration in Chlamydomonas. Proc. Natl. Acad. Sci. USA **108:** 20820–20825.

Ibrahim, F., Rymarquis, L.A., Kim, E.J., Becker, J., Balassa, E., Green, P.J., and Cerutti, H. (2010). Uridylation of mature miRNAs and siRNAs by the MUT68 nucleotidyltransferase promotes their degradation in Chlamydomonas. Proc. Natl. Acad. Sci. USA **107:** 3906–3911.

Johnson, X., Wostrikoff, K., Finazzi, G., Kuras, R., Schwarz, C., Bujaldon, S., Nickelsen, J., Stern, D.B., Wollman, F.A., and Vallon, O. (2010). MRL1, a conserved pentatricopeptide repeat protein, is required for stabilization of rbcL mRNA in Chlamydomonas and Arabidopsis. Plant Cell **22:** 234–248.

Kanekatsu, M., Ezumi, A., Nakamura, T., and Ohtsuki, K. (1995). Chloroplast ribonucleoproteins (RNPs) as phosphate acceptors for casein kinase II: purification by ssDNA-cellulose column chromatography. Plant Cell Physiol. **36:** 1649–1656.

Kanekatsu, M., Saito, H., Motohashi, K., and Hisabori, T. (1998). The beta subunit of chloroplast ATP synthase (CF0CF1-ATPase) is phosphorylated by casein kinase II. Biochem. Mol. Biol. Int. **46:** 99–105.

Ke, J., Chen, R.Z., Ban, T., Zhou, X.E., Gu, X., Tan, M.H., Chen, C., Kang, Y., Brunzelle, J.S., Zhu, J.K., Melcher, K., and Xu, H.E. (2013). Structural basis for RNA recognition by a dimeric PPR-protein complex. Nat. Struct. Mol. Biol. **20:** 1377–1382.

Kinoshita, E., and Kinoshita-Kikuta, E. (2011). Improved Phos-tag SDS-PAGE under neutral pH conditions for advanced protein phosphorylation profiling. Proteomics **11:** 319–323.

Kinoshita, E., Kinoshita-Kikuta, E., Takiyama, K., and Koike, T. (2006). Phosphate-binding tag, a new tool to visualize phosphorylated proteins. Mol. Cell. Proteomics **5:** 749–757.

Klinkert, B., Schwarz, C., Pohlmann, S., Pierre, Y., Girard-Bascou, J., and Nickelsen, J. (2005). Relationship between mRNA levels and protein accumulation in a chloroplast promoter-mutant of *Chlamydomonas reinhardtii*. Mol. Genet. Genomics **274:** 637–643.

Kropat, J., Hong-Hermesdorf, A., Casero, D., Ent, P., Castruita, M., Pellegrini, M., Merchant, S.S., and Malasarn, D. (2011). A revised mineral nutrient supplement increases biomass and growth rate in *Chlamydomonas reinhardtii*. Plant J. **66:** 770–780.

Kuchka, M.R., Goldschmidt-Clermont, M., van Dillewijn, J., and Rochaix, J.D. (1989). Mutation at the Chlamydomonas nuclear NAC2 locus specifically affects stability of the chloroplast psbD transcript encoding polypeptide D2 of PS II. Cell **58:** 869–876.

Kück, U., Choquet, Y., Schneider, M., Dron, M., and Bennoun, P. (1987). Structural and transcription analysis of two homologous genes for the P700 chlorophyll a-apoproteins in *Chlamydomonas reinhardii*: evidence for in vivo trans-splicing. EMBO J. **6:** 2185–2195.

Kupsch, C., Ruwe, H., Gusewski, S., Tillich, M., Small, I., and Schmitz-Linneweber, C. (2012). Arabidopsis chloroplast RNA binding proteins CP31A and CP29A associate with large transcript pools and confer cold stress tolerance by influencing multiple chloroplast RNA processing steps. Plant Cell **24:** 4266–4280.

Lefebvre-Legendre, L., Choquet, Y., Kuras, R., Loubery, S., Douchi, D., and Goldschmidt-Clermont, M. (2015). A nucleus-encoded chloroplast protein regulated by iron availability governs expression of the photosystem I subunit PsaA in *Chlamydomonas reinhardtii*. Plant Physiol. **167:** 1527–1540.

Lefebvre-Legendre, L., Merendino, L., Rivier, C., and Goldschmidt-Clermont, M. (2014). On the complexity of chloroplast RNA metabolism: psaA trans-splicing can be bypassed in Chlamydomonas. Mol. Biol. Evol. **31:** 2697–2707.

Lefebvre, P.A., and Silflow, C.D. (1999). Chlamydomonas: the cell and its genomes. Genetics **151:** 9–14.

Lemeille, S., and Rochaix, J.D. (2010). State transitions at the crossroad of thylakoid signalling pathways. Photosynth. Res. **106:** 33–46.

Liere, K., and Link, G. (1997). Chloroplast endoribonuclease p54 involved in RNA 3′-end processing is regulated by phosphorylation and redox state. Nucleic Acids Res. **25:** 2403–2408.

Lisitsky, I., and Schuster, G. (1995). Phosphorylation of a chloroplast RNA-binding protein changes its affinity to RNA. Nucleic Acids Res. **23:** 2506–2511.

Lohrig, K., Müller, B., Davydova, J., Leister, D., and Wolters, D.A. (2009). Phosphorylation site mapping of soluble proteins: bioinformatical filtering reveals potential plastidic phosphoproteins in *Arabidopsis thaliana*. Planta **229:** 1123–1134.

Loiselay, C., Gumpel, N.J., Girard-Bascou, J., Watson, A.T., Purton, S., Wollman, F.A., and Choquet, Y. (2008). Molecular identification and function of cis- and trans-acting determinants for petA transcript stability in *Chlamydomonas reinhardtii* chloroplasts. Mol. Cell. Biol. **28:** 5529–5542.

Loizeau, K., Qu, Y., Depp, S., Fiechter, V., Ruwe, H., Lefebvre-Legendre, L., Schmitz-Linneweber, C., and Goldschmidt-Clermont, M. (2014). Small RNAs reveal two target sites of the RNA-maturation factor Mbb1 in the chloroplast of Chlamydomonas. Nucleic Acids Res. **42:** 3286–3297.

Longoni, P., Douchi, D., Cariti, F., Fucile, G., and Goldschmidt-Clermont, M. (2015). Phosphorylation of the light-harvesting complex II isoform Lhcb2 is central to state transitions. Plant Physiol. **169:** 2874–2883.

Lukeš, J., Archibald, J.M., Keeling, P.J., Doolittle, W.F., and Gray, M.W. (2011). How a neutral evolutionary ratchet can build cellular complexity. IUBMB Life **63:** 528–537.

Maier, U.G., Bozarth, A., Funk, H.T., Zauner, S., Rensing, S.A., Schmitz-Linneweber, C., Börner, T., and Tillich, M. (2008). Complex chloroplast RNA metabolism: just debugging the genetic programme? BMC Biol. **6:** 36.

Matsuo, T., Onai, K., Okamoto, K., Minagawa, J., and Ishiura, M. (2006). Real-time monitoring of chloroplast gene expression by a luciferase reporter: evidence for nuclear regulation of chloroplast circadian period. Mol. Cell. Biol. **26:** 863–870.

Michelet, L., Lefebvre-Legendre, L., Burr, S.E., Rochaix, J.D., and Goldschmidt-Clermont, M. (2011). Enhanced chloroplast transgene expression in a nuclear mutant of Chlamydomonas. Plant Biotechnol. J. **9:** 565–574.

Monod, C., Goldschmidt-Clermont, M., and Rochaix, J.D. (1992). Accumulation of chloroplast psbB RNA requires a nuclear factor in *Chlamydomonas reinhardtii*. Mol. Gen. Genet. **231:** 449–459.

Moseley, J.L., Allinger, T., Herzog, S., Hoerth, P., Wehinger, E., Merchant, S., and Hippler, M. (2002). Adaptation to Fe-deficiency requires remodeling of the photosynthetic apparatus. EMBO J. **21:** 6709–6720.

Naumann, B., Stauber, E.J., Busch, A., Sommer, F., and Hippler, M. (2005). N-terminal processing of Lhca3 Is a key step in remodeling of the photosystem I-light-harvesting complex under iron deficiency in *Chlamydomonas reinhardtii*. J. Biol. Chem. **280:** 20431–20441.

Naver, H., Boudreau, E., and Rochaix, J.D. (2001). Functional studies of Ycf3: its role in assembly of photosystem I and interactions with some of its subunits. Plant Cell **13:** 2731–2745.

Nickelsen, J., Fleischmann, M., Boudreau, E., Rahire, M., and Rochaix, J.D. (1999). Identification of cis-acting RNA leader elements required for chloroplast psbD gene expression in Chlamydomonas. Plant Cell **11:** 957–970.

Ozawa, S., Nield, J., Terao, A., Stauber, E.J., Hippler, M., Koike, H., Rochaix, J.D., and Takahashi, Y. (2009). Biochemical and structural studies of the large Ycf4-photosystem I assembly complex of the green alga *Chlamydomonas reinhardtii*. Plant Cell **21:** 2424–2442.

Pfalz, J., Bayraktar, O.A., Prikryl, J., and Barkan, A. (2009). Site-specific binding of a PPR protein defines and stabilizes 5′ and 3′ mRNA termini in chloroplasts. EMBO J. **28:** 2042–2052.

Preker, P.J., and Keller, W. (1998). The HAT helix, a repetitive motif implicated in RNA processing. Trends Biochem. Sci. **23:** 15–16.

Prikryl, J., Rojas, M., Schuster, G., and Barkan, A. (2011). Mechanism of RNA stabilization and translational activation by a pentatricopeptide repeat protein. Proc. Natl. Acad. Sci. USA **108:** 415–420.

Puthiyaveetil, S., Kavanagh, T.A., Cain, P., Sullivan, J.A., Newell, C.A., Gray, J.C., Robinson, C., van der Giezen, M., Rogers, M.B., and Allen, J.F. (2008). The ancestral symbiont sensor kinase CSK links photosynthesis with gene expression in chloroplasts. Proc. Natl. Acad. Sci. USA **105:** 10061–10066.

Rahire, M., Laroche, F., Cerutti, L., and Rochaix, J.D. (2012). Identification of an OPR protein involved in the translation initiation of the PsaB subunit of photosystem I. Plant J. **72:** 652–661.

Ramundo, S., Rahire, M., Schaad, O., and Rochaix, J.D. (2013). Repression of essential chloroplast genes reveals new signaling pathways and regulatory feedback loops in Chlamydomonas. Plant Cell **25:** 167–186.

Raynaud, C., Loiselay, C., Wostrikoff, K., Kuras, R., Girard-Bascou, J., Wollman, F.A., and Choquet, Y. (2007). Evidence for regulatory function of nucleus-encoded factors on mRNA stabilization and translation in the chloroplast. Proc. Natl. Acad. Sci. USA **104:** 9093–9098.

Redding, K. (2009). Photosystem I. In The Chlamydomonas Sourcebook, D. Stern, ed (Oxford, UK: Academic Press), pp. 541–572.

Redding, K., MacMillan, F., Leibl, W., Brettel, K., Hanley, J., Rutherford, A.W., Breton, J., and Rochaix, J.D. (1998). A systematic survey of conserved histidines in the core subunits of Photosystem I by site-directed mutagenesis reveals the likely axial ligands of P700. EMBO J. **17:** 50–60.

Reiland, S., Finazzi, G., Endler, A., Willig, A., Baerenfaller, K., Grossmann, J., Gerrits, B., Rutishauser, D., Gruissem, W., Rochaix, J.D., and Baginsky, S. (2011). Comparative phosphoproteome profiling reveals a function of the STN8 kinase in fine-tuning of cyclic electron flow (CEF). Proc. Natl. Acad. Sci. USA **108:** 12955–12960.

Reiland, S., Messerli, G., Baerenfaller, K., Gerrits, B., Endler, A., Grossmann, J., Gruissem, W., and Baginsky, S. (2009). Large-scale Arabidopsis phosphoproteome profiling reveals novel chloroplast kinase substrates and phosphorylation networks. Plant Physiol. **150:** 889–903.

Rio, D.C., Hannon, G.J., and Nilsen, T.W. (2011). RNA: A Laboratory Manual. (Cold Spring Harbor, NY: Cold Spring Harbor Laboratory Press).

Rivier, C., Goldschmidt-Clermont, M., and Rochaix, J.D. (2001). Identification of an RNA-protein complex involved in chloroplast group II intron trans-splicing in *Chlamydomonas reinhardtii*. EMBO J. **20:** 1765–1773.

Ruwe, H., and Schmitz-Linneweber, C. (2012). Short non-coding RNA fragments accumulating in chloroplasts: footprints of RNA binding proteins? Nucleic Acids Res. **40:** 3106–3116.

Sambrook, J., Fritsch, E.F., and Maniatis, T. (1989). Molecular Cloning. A Laboratory Manual. (Cold Spring Harbor, NY: Cold Spring Harbor Laboratory Press).

Sane, A.P., Stein, B., and Westhoff, P. (2005). The nuclear gene HCF107 encodes a membrane-associated R-TPR (RNA tetratricopeptide repeat)-containing protein involved in expression of the plastidial psbH gene in Arabidopsis. Plant J. **42:** 720–730.

Schmitz-Linneweber, C., Kushnir, S., Babiychuk, E., Poltnigg, P., Herrmann, R.G., and Maier, R.M. (2005a). Pigment deficiency in nightshade/tobacco cybrids is caused by the failure to edit the plastid ATPase alpha-subunit mRNA. Plant Cell **17:** 1815–1828.

Schmitz-Linneweber, C., Williams-Carrier, R., and Barkan, A. (2005b). RNA immunoprecipitation and microarray analysis show a chloroplast Pentatricopeptide repeat protein to be associated with the 5′ region of mRNAs whose translation it activates. Plant Cell **17:** 2791–2804.

Schweer, J., Türkeri, H., Kolpack, A., and Link, G. (2010). Role and regulation of plastid sigma factors and their functional interactors during chloroplast transcription - recent lessons from *Arabidopsis thaliana*. Eur. J. Cell Biol. **89:** 940–946.

Shimogawara, K., Fujiwara, S., Grossman, A., and Usuda, H. (1998). High-efficiency transformation of *Chlamydomonas reinhardtii* by electroporation. Genetics **148:** 1821–1828.

Stampacchia, O., Girard-Bascou, J., Zanasco, J.L., Zerges, W., Bennoun, P., and Rochaix, J.D. (1997). A nuclear-encoded function essential for translation of the chloroplast psaB mRNA in Chlamydomonas. Plant Cell **9:** 773–782.

Stern, D.B., Goldschmidt-Clermont, M., and Hanson, M.R. (2010). Chloroplast RNA metabolism. Annu. Rev. Plant Biol. **61:** 125–155.

Takahashi, Y., Goldschmidt-Clermont, M., Soen, S.Y., Franzén, L.G., and Rochaix, J.D. (1991). Directed chloroplast transformation in *Chlamydomonas reinhardtii*: insertional inactivation of the psaC gene encoding the iron sulfur protein destabilizes photosystem I. EMBO J. **10:** 2033–2040.

Takahashi, Y., Matsumoto, H., Goldschmidt-Clermont, M., and Rochaix, J.D. (1994). Directed disruption of the Chlamydomonas chloroplast psbK gene destabilizes the photosystem II reaction center complex. Plant Mol. Biol. **24:** 779–788.

Tamura, K., Stecher, G., Peterson, D., Filipski, A., and Kumar, S. (2013). MEGA6: Molecular Evolutionary Genetics Analysis version 6.0. Mol. Biol. Evol. **30:** 2725–2729.

Terauchi, A.M., Peers, G., Kobayashi, M.C., Niyogi, K.K., and Merchant, S.S. (2010). Trophic status of *Chlamydomonas reinhardtii* influences the impact of iron deficiency on photosynthesis. Photosynth. Res. **105:** 39–49.

Tikkanen, M., Nurmi, M., Kangasjärvi, S., and Aro, E.M. (2008). Core protein phosphorylation facilitates the repair of photodamaged photosystem II at high light. Biochim. Biophys. Acta **1777:** 1432–1437.

Urzica, E.I., Casero, D., Yamasaki, H., Hsieh, S.I., Adler, L.N., Karpowicz, S.J., Blaby-Haas, C.E., Clarke, S.G., Loo, J.A., Pellegrini, M., and Merchant, S.S. (2012). Systems and trans-system level analysis identifies conserved iron deficiency responses in the plant lineage. Plant Cell **24:** 3921–3948.

Urzica, E.I., Vieler, A., Hong-Hermesdorf, A., Page, M.D., Casero, D., Gallaher, S.D., Kropat, J., Pellegrini, M., Benning, C., and Merchant, S.S. (2013). Remodeling of membrane lipids in iron-starved Chlamydomonas. J. Biol. Chem. **288:** 30246–30258.

Vaistij, F.E., Boudreau, E., Lemaire, S.D., Goldschmidt-Clermont, M., and Rochaix, J.D. (2000a). Characterization of Mbb1, a nucleus-encoded tetratricopeptide-like repeat protein required for expression of the chloroplast psbB/psbT/psbH gene cluster in *Chlamydomonas reinhardtii*. Proc. Natl. Acad. Sci. USA **97:** 14813–14818.

Vaistij, F.E., Goldschmidt-Clermont, M., Wostrikoff, K., and Rochaix, J.D. (2000b). Stability determinants in the chloroplast psbB/T/H mRNAs of *Chlamydomonas reinhardtii*. Plant J. **21:** 469–482.

Wang, F., Johnson, X., Cavaiuolo, M., Bohne, A.V., Nickelsen, J., and Vallon, O. (2015). Two Chlamydomonas OPR proteins stabilize chloroplast mRNAs encoding small subunits of photosystem II and cytochrome b6 f. Plant J. **82:** 861–873.

Wang, H., Gau, B., Slade, W.O., Juergens, M., Li, P., and Hicks, L.M. (2014). The global phosphoproteome of *Chlamydomonas reinhardtii* reveals complex organellar phosphorylation in the flagella and thylakoid membrane. Mol. Cell. Proteomics **13:** 2337–2353.

Wei, L., Derrien, B., Gautier, A., Houille-Vernes, L., Boulouis, A., Saint-Marcoux, D., Malnoë, A., Rappaport, F., de Vitry, C., Vallon, O., Choquet, Y., and Wollman, F.A. (2014). Nitric oxide-triggered remodeling of chloroplast bioenergetics and thylakoid proteins upon nitrogen starvation in *Chlamydomonas reinhardtii*. Plant Cell **26:** 353–372.

Wessel, D., and Flügge, U.I. (1984). A method for the quantitative recovery of protein in dilute solution in the presence of detergents and lipids. Anal. Biochem. **138:** 141–143.

Williams-Carrier, R., Kroeger, T., and Barkan, A. (2008). Sequence-specific binding of a chloroplast pentatricopeptide repeat protein to its native group II intron ligand. RNA **14:** 1930–1941.

Wollman, F.A., and Delepelaire, P. (1984). Correlation between changes in light energy distribution and changes in thylakoid membrane polypeptide phosphorylation in *Chlamydomonas reinhardtii*. J. Cell Biol. **98:** 1–7.

Wostrikoff, K., Girard-Bascou, J., Wollman, F.A., and Choquet, Y. (2004). Biogenesis of PSI involves a cascade of translational autoregulation in the chloroplast of Chlamydomonas. EMBO J. **23:** 2696–2705.

Yin, P., et al. (2013). Structural basis for the modular recognition of single-stranded RNA by PPR proteins. Nature **504:** 168–171.

Zhelyazkova, P., Hammani, K., Rojas, M., Voelker, R., Vargas-Suárez, M., Börner, T., and Barkan, A. (2012). Protein-mediated protection as the predominant mechanism for defining processed mRNA termini in land plant chloroplasts. Nucleic Acids Res. **40:** 3092–3105.

A Nucleus-Encoded Chloroplast Phosphoprotein Governs Expression of the Photosystem I Subunit PsaC in *Chlamydomonas reinhardtii*

Damien Douchi, Yujiao Qu, Paolo Longoni, Linnka Legendre-Lefebvre, Xenie Johnson, Christian Schmitz-Linneweber and Michel Goldschmidt-Clermont

Plant Cell 2016;28;1182-1199; originally published online April 25, 2016;
DOI 10.1105/tpc.15.00725